A6180/8180:
Modern Scattering Methods in Materials Science

Lecture given by Prof. Tamas UNGAR

Office: G6601
E-mail: tungar@cityu.edu.hk
Course leader: Dr Suresh M. Chathoth

Structure determination by diffraction

香港城市大學
City University
of Hong Kong

Structure determination by diffraction,

powder diffraction,

systematic extinction,

indexing,

Patterson function

phase analysis,

data-bases and applications,

Rietveld analysis,

special applications,

stress-strain

texture determination,

line profile analysis

indexing

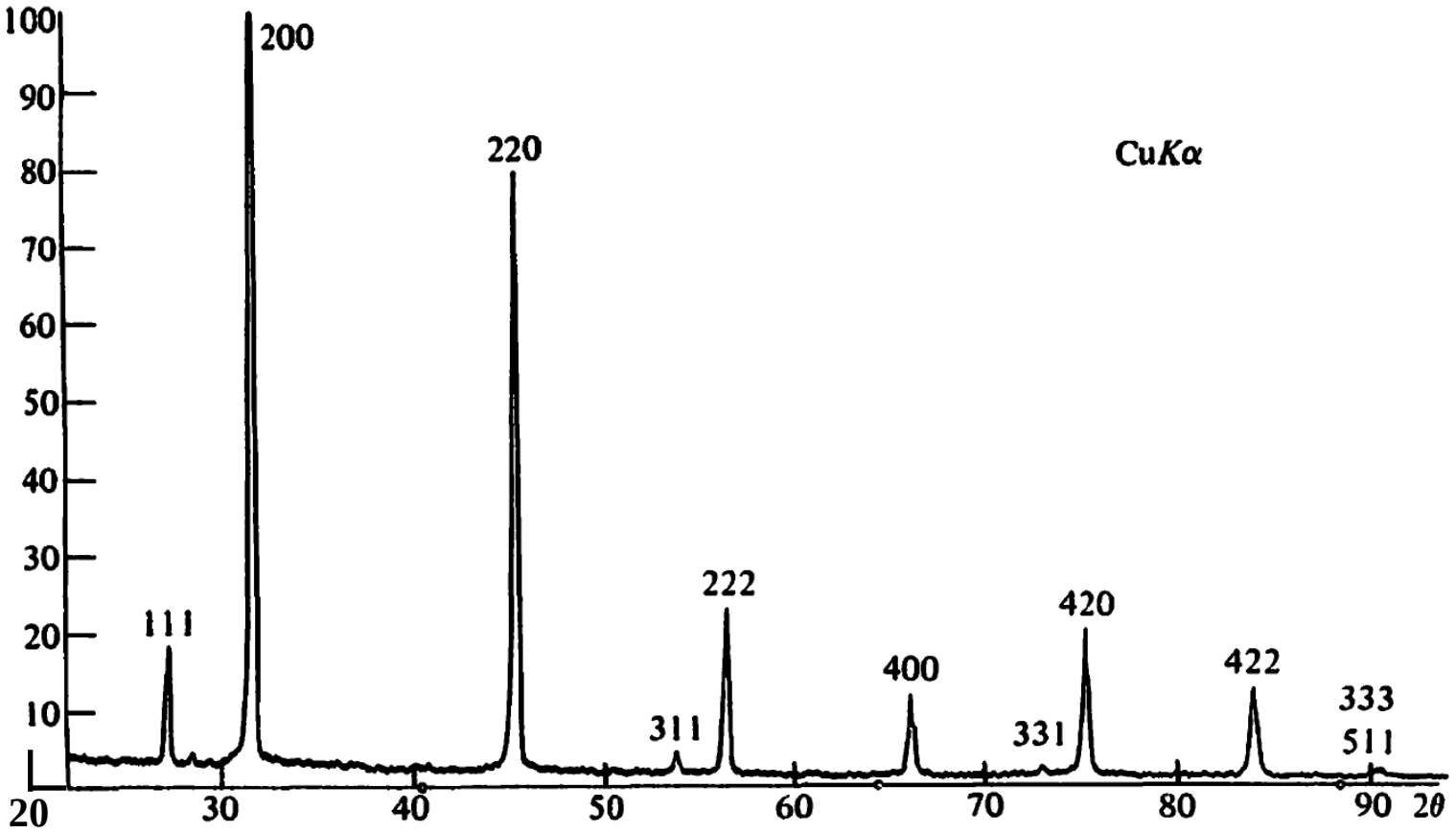

Fig. 5.6 Diffractometer recording of the powder pattern of using Ni filtered Cu*K*α radiation.

indexing

when the crystal system is unknown

we would start out by

trying to index the pattern in terms of a cubic lattice

If it is not cubic, this

will quickly turn out to be impossible,

and we would then fall back on the

various schemes for handling systems of lower symmetry

for a cubic crystal

$$\frac{4 \sin^2 \theta}{\lambda^2} = \frac{1}{d^2} = \frac{h^2 + k^2 + l^2}{a^2}$$

Warren, X-ray Diffraction

indexing

1	2
2θ	$\frac{4\sin^2\theta}{\lambda^2}$
27.3	0.0940
31.7	0.1255
45.5	0.2516
53.9	0.3455
56.5	0.3768
66.3	0.503
73.2	0.598
75.4	0.629
84.1	0.755
90.6	0.849

1) divide #2 by 0.0940

2) divide #2 by $\frac{0.0940}{2}$

3) divide #2 by $\frac{0.0940}{3}$

etc.

Warren, X-ray Diffraction

indexing

column #3 from #2

	3
	$h^2 + k^2 + l^2$
3	3
4.0053	4
8.02978	8
11.0265	11
12.0255	12
16.053	16
19.085	19
20.0744	20
24.0957	24
27.0957	27

Warren, X-ray Diffraction

indexing and structure from a powder pattern

POWDER DIFFRACTOMETER PATTERN OF NaCl ($\lambda = 1.542$ A)

1	2	3	4	5	6	7	8	9	10	11	12	13	14
2θ	$\frac{4\sin^2\theta}{\lambda^2}$	$h^2+k^2+l^2$	hkl	$a(A)$	$\frac{\sin\theta}{\lambda}$	f_{Cl}	f_{Na}	F^2	m	(LP)	$\frac{F^2m(LP)}{1000}$	A, arb. unit	Col. 12 corrected
27.3	0.0940	3	111	5.65	0.154	13.50	8.90	338	8	33.5	91	116	102
31.7	0.1255	4	200	5.65	0.177	12.70	8.70	7330	6	24.0	1057	1260	1160
45.5	0.2516	8	220	5.64	0.251	10.50	7.65	5280	12	10.9	690	694	697
53.9	0.3455	11	311	5.64	0.294	9.60	7.00	107	24	7.4	19	23	18
56.5	0.3768	12	222	5.64	0.307	9.35	6.75	4150	8	6.6	219	200	201
66.3	0.503	16	400	5.64	0.354	8.65	6.10	3490	6	4.7	98	92	82
73.2	0.598	19	331	5.64	0.386	8.30	5.65	112	24	3.8	10	13	8
75.4	0.629	20	420	5.64	0.396	8.20	5.50	3010	24	3.60	260	198	195
84.1	0.755	24	422	5.64	0.434	7.85	5.05	2660	24	3.05	195	136	136
90.6	0.849	27	511 333	5.64	0.461	7.60	4.75	130	24 8	2.80	12	10	8

香港城市大學
City University of Hong Kong

Warren, X-ray Diffraction

indexing and structure from a powder pattern

columns #7 and #8

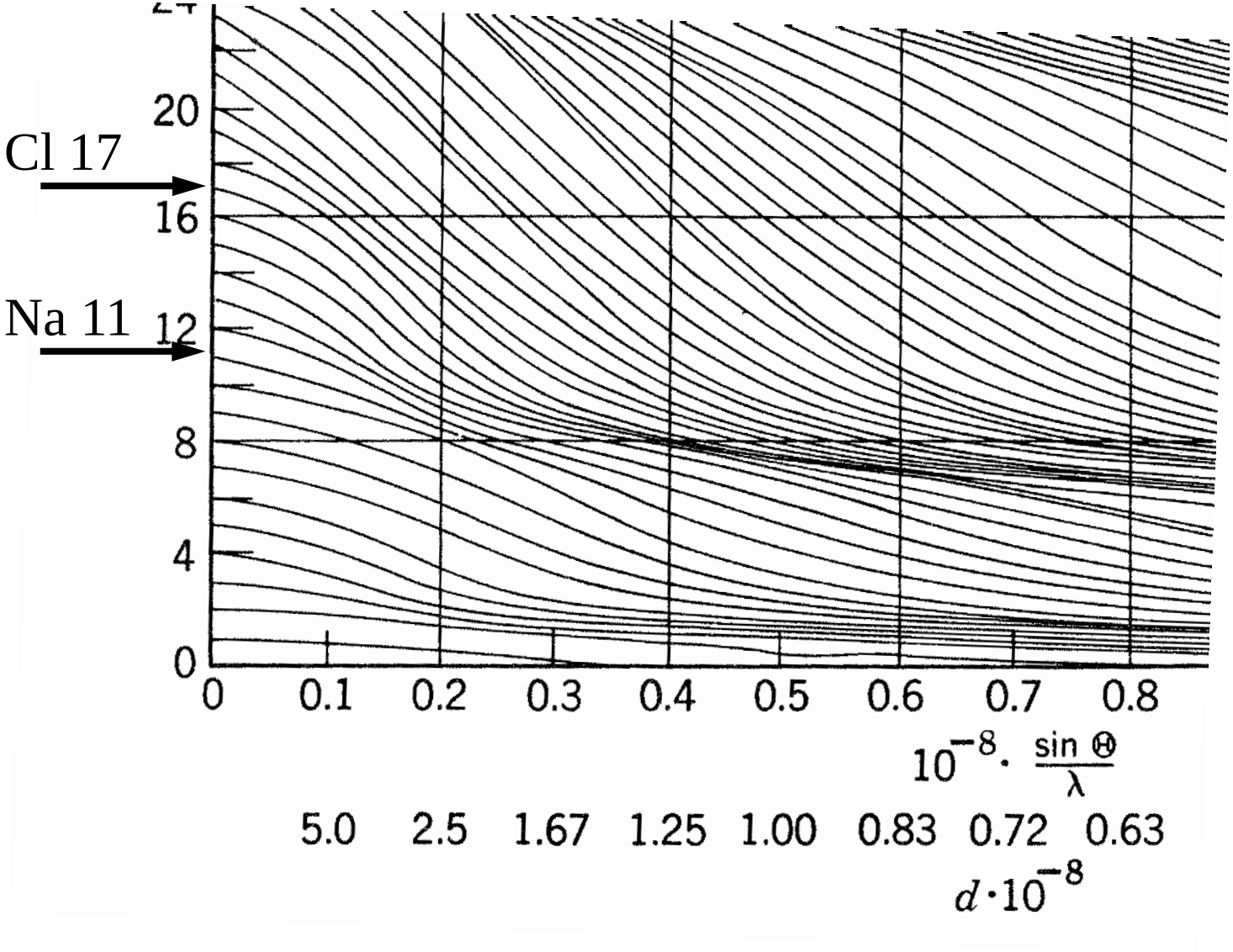

Warren, X-ray Diffraction

indexing and structure from a powder pattern

column #9

The number of Na and Cl atoms per unit cell

the mass of the unit cell

$$n = \frac{N\rho a^3}{M} = \frac{0.602 \times 10^{24} \times 2.17 \times (5.64 \times 10^{-8})^3}{(23.0 + 35.5)} = 4.00$$

M: Na Cl

4 Na and 4 Cl per cubic unit cell

---

we can choose the coordinates of the 4 Cl atoms as: **0 0 0, ½ ½ 0, ½ 0 ½, 0 ½ ½**

---

where to put the Na atoms?

if one Na is at: x,y,z, then the other 3 are fixed

for the first position there are 3 possibilities in a cubic lattice:

½ ½ ½; ¼ ¼ ¼; and ¾ ¾ ¾ but only the first 2 are different

---

we can start with the first option: **½ ½ ½**

indexing and structure from a powder pattern

LP : Lorentz-Polarization factor

polarization factor $\dfrac{1 + \cos^2 2\theta}{2}$

Lorentz - polarization factor

for an unpolarized incoming beam

$$\frac{1 + \cos^2 2\theta}{\sin \theta \sin 2\theta}$$

Warren, X-ray Diffraction

indexing and structure from a powder pattern

indexing NaCl as ZnS

from the two options: $\frac{1}{2}\frac{1}{2}\frac{1}{2}$; $\frac{1}{4}\frac{1}{4}\frac{1}{4}$;

checking with the other option: $\frac{1}{4}\frac{1}{4}\frac{1}{4}$

INTERPRETATION OF NaCl PATTERN IN TERMS OF ZINC BLENDE STRUCTURE

hkl	f_{Cl}	f_{Na}	F^2	*m*	(LP)	$\frac{F^2 m(LP)}{1000}$	*A* arb. units
111	13.50	8.90	4180	8	33.5	1120	116
200	12.70	8.70	256	6	24.0	37	1260
220	10.50	7.65	5270	12	10.9	690	694

the **intensities turn out** to be **wrong**

香港城市大學 City University of Hong Kong

Warren, X-ray Diffraction

indexing and structure from a powder pattern

Na Cl

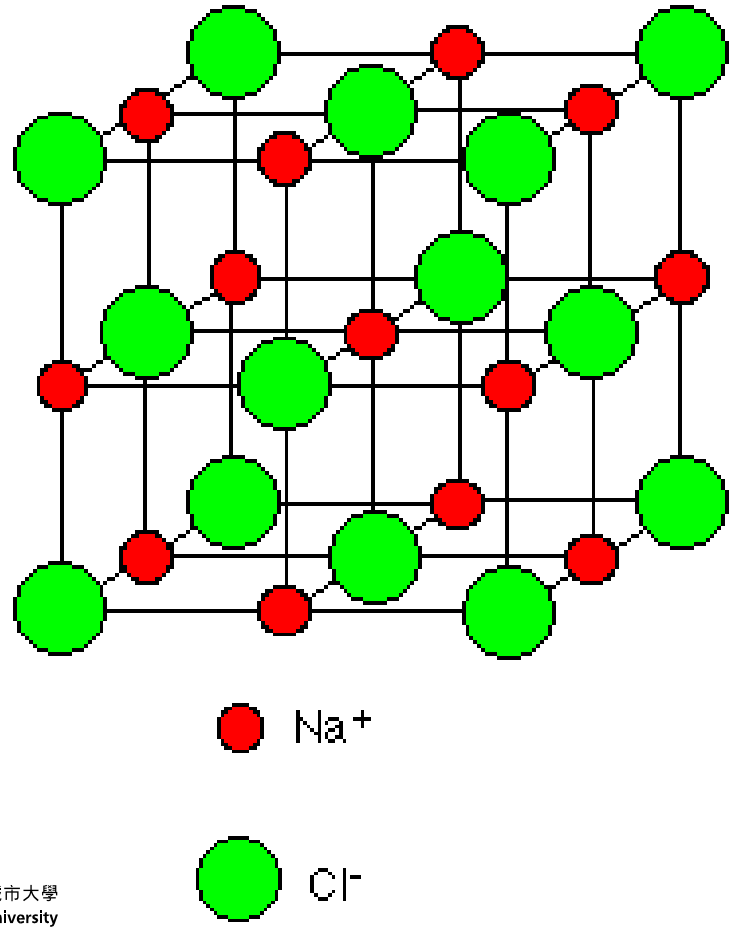

ZnS

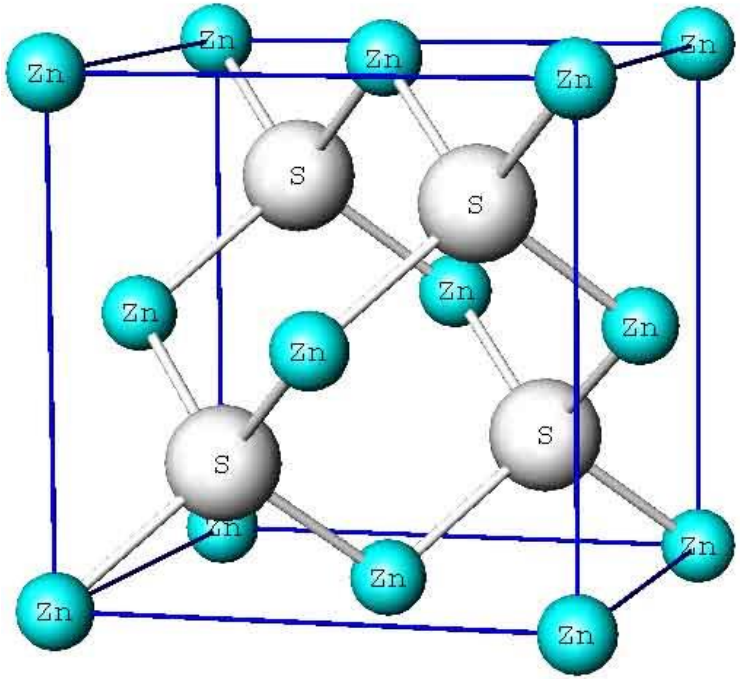

Structure determination by diffraction,

powder diffraction,

systematic extinction,

indexing,

Patterson function

---

phase analysis,

data-bases and applications,

Rietveld analysis,

special applications,

stress-strain

texture determination,

line profile analysis

Patterson function

the atomic scattering factor:

$$f_n = \int 4\pi r^2 \rho_n(r) \frac{\sin kr}{kr} dr$$

structure factor:

$$F_{hkl} = \sum_n f_n e^{2\pi i(hx_n + ky_n + lz_n)}$$

the structure factor in terms of continuous electron/charge density:

$$F_{khl} = \int_0^a \int_0^b \int_0^c \rho(xyz) e^{2\pi i[h(x/a)+k(y/b)+l(z/c)]} dV$$

this is a Fourier transform:

$$F_{hkl} = \mathrm{FT}[\rho(\mathbf{r})]$$

The scattered intensity: $I(\mathbf{K}) = |F_{hkl}|^2$, where $\mathrm{K} = \frac{2sin\theta}{\lambda}$

Patterson function

$$|F_{hkl}|^2 = F_{hkl} \times F_{hkl}^* = \mathrm{FT}[\rho(\mathbf{r})] \times \mathrm{FT}[\rho(-\mathbf{r})] =$$

$$= \mathrm{FT}[\rho(\mathbf{r}) * \rho(-\mathbf{r})] = \mathrm{FT}[P(\mathbf{r})]$$

$$P(\mathbf{r}) = \int \rho(\mathbf{r})\rho(\mathbf{r} + \mathbf{r}')d^3\mathbf{r}'$$

Patterson function: autocorrelation of $\rho(\mathbf{r})$

Patterson function

linear charge density and the corresponding Patterson function

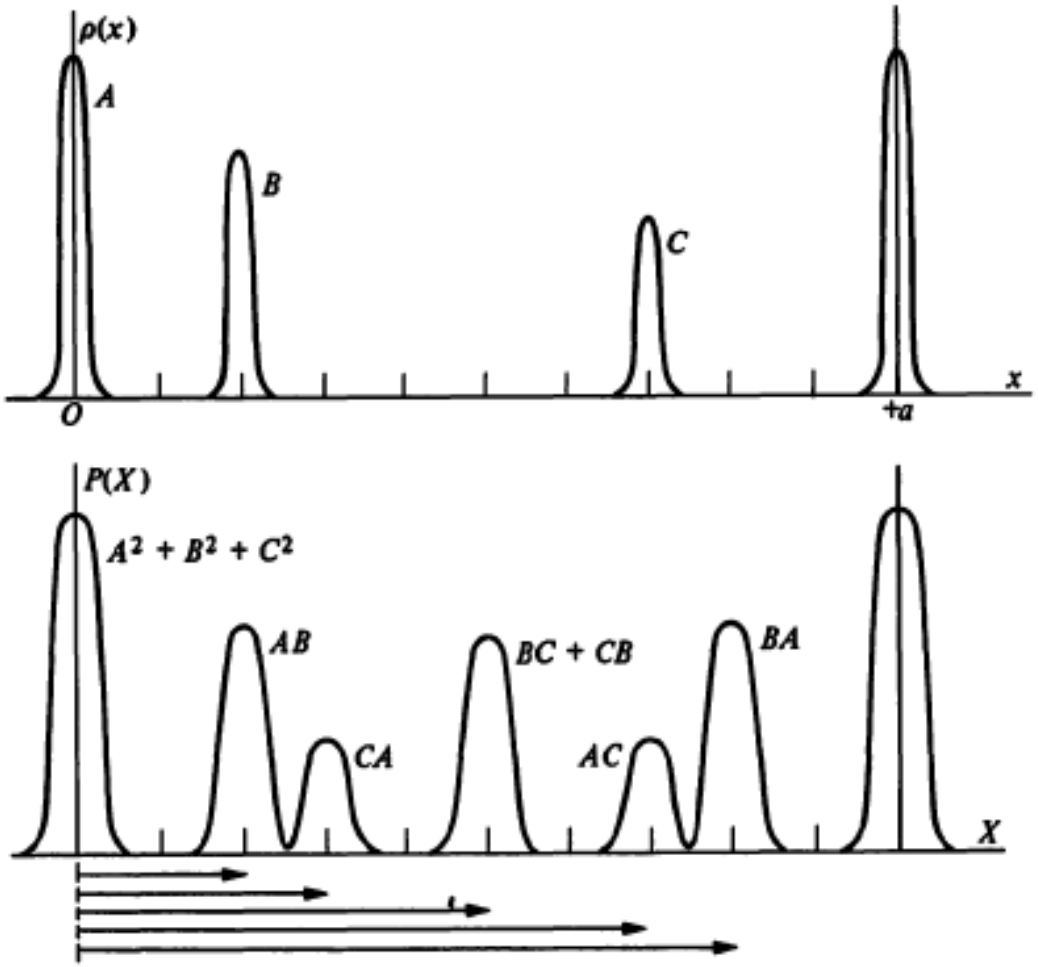

Patterson function

a diffraction experiment yields: the **pair - correlation**

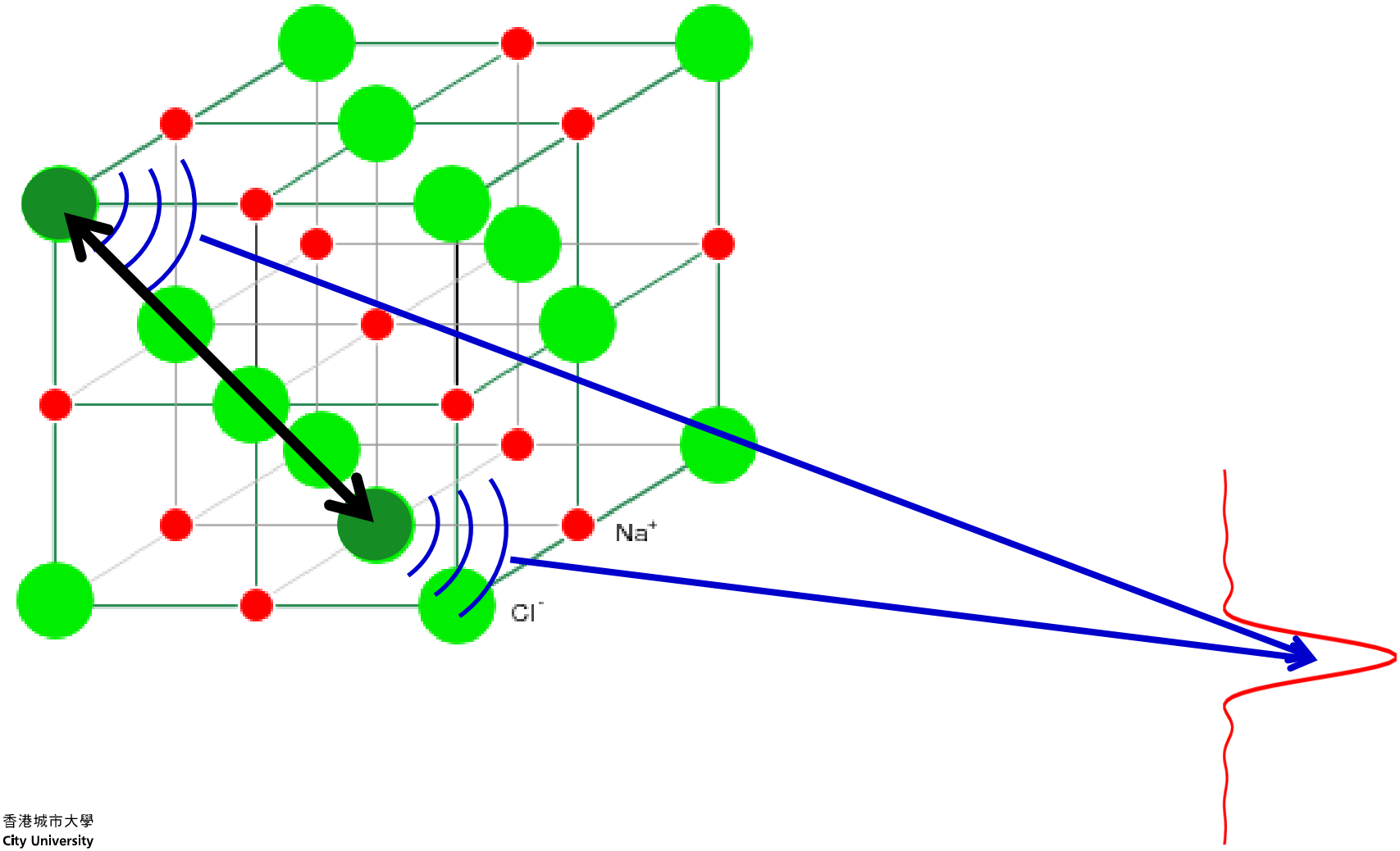

Structure determination by diffraction,

powder diffraction,

systematic extinction,

indexing,

Patterson function

phase analysis,

data-bases and applications,

Rietveld analysis,

special applications,

stress-strain

texture determination,

line profile analysis

phase analysis, data – bases

a diffraction pattern is the **fingerprint** of materials

Identification of unknown phases

Search / Match

- Powder data : unique
- Identification : d , I
- d : decreasing intensity

search in Powder Diffraction File PDF
until match is obtained

- continued until all lines and phases identified
- Hanawalt method : 3 strongest lines

phase analysis, data – bases

a diffraction pattern is the **fingerprint** of materials

- alternative methods

  reduced powder pattern : "stick" diagram

  d – I pairs

  ICDD data bank : 1996 >55.000

- Johnson – Vand phase identification
  - data collection
  - data reduction : background ; α doublett
  - determination of maxima
  - search in ICDD data file by d-I pairs

ICDD data files

PDF # 461212, Wavelength = 1.540562 (A)

46-1212 Quality: *

CAS Number:

Molecular Weight: 101.96
Volume[CD]: 254.81
Dx: 3.987 Dm:

Sys: Hexagonal
Lattice: Rhomb-centered
S.G.: R$\bar{3}$c (167)
Cell Parameters:
a 4.758 b c 12.99
α β γ

SS/FOM: F25=358(.0028, 25)
I/Icor:
Rad: CuKa1
Lambda: 1.540562
Filter:
d-sp: diffractometer

Mineral Name:
Corundum, syn

α-Al2 O3
Aluminum Oxide
Ref: Huang, T et al., Adv. X-Ray Anal., 33, 295 (1990)

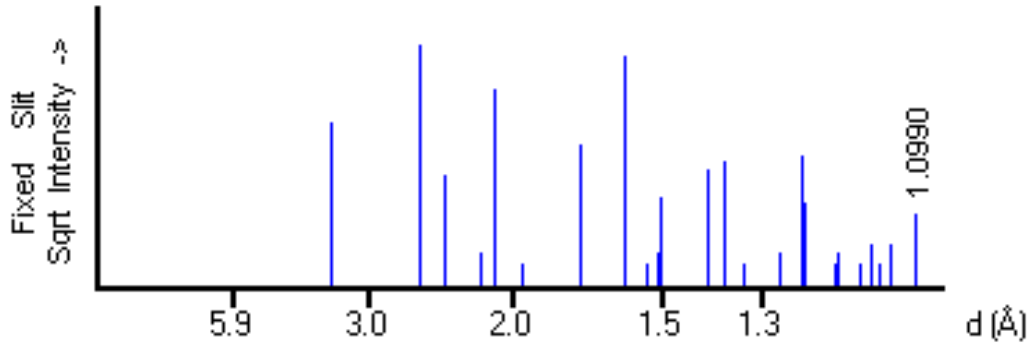

d(A)	Int-f	h	k	l	d(A)	Int-f	h	k	l	d(A)	Int-f	h	k	l
3.4797	45	0	1	2	1.5150	2	1	2	2	1.1897	2	2	2	0
2.5508	100	1	0	4	1.5110	14	0	1	8	1.1600	1	3	0	6
2.3794	21	1	1	0	1.4045	23	2	1	4	1.1472	3	2	2	3
2.1654	2	0	0	6	1.3737	27	3	0	0	1.1386	<1	1	3	1
2.0853	66	1	1	3	1.3359	1	1	2	5	1.1256	2	3	1	2
1.9643	1	2	0	2	1.2755	2	2	0	8	1.1241	3	1	2	8
1.7400	34	0	2	4	1.2391	29	1	0	10	1.0990	9	0	2	10
1.6015	89	1	1	6	1.2343	12	1	1	9					
1.5466	1	2	1	1	1.1931	1	2	1	7					

ICDD data files

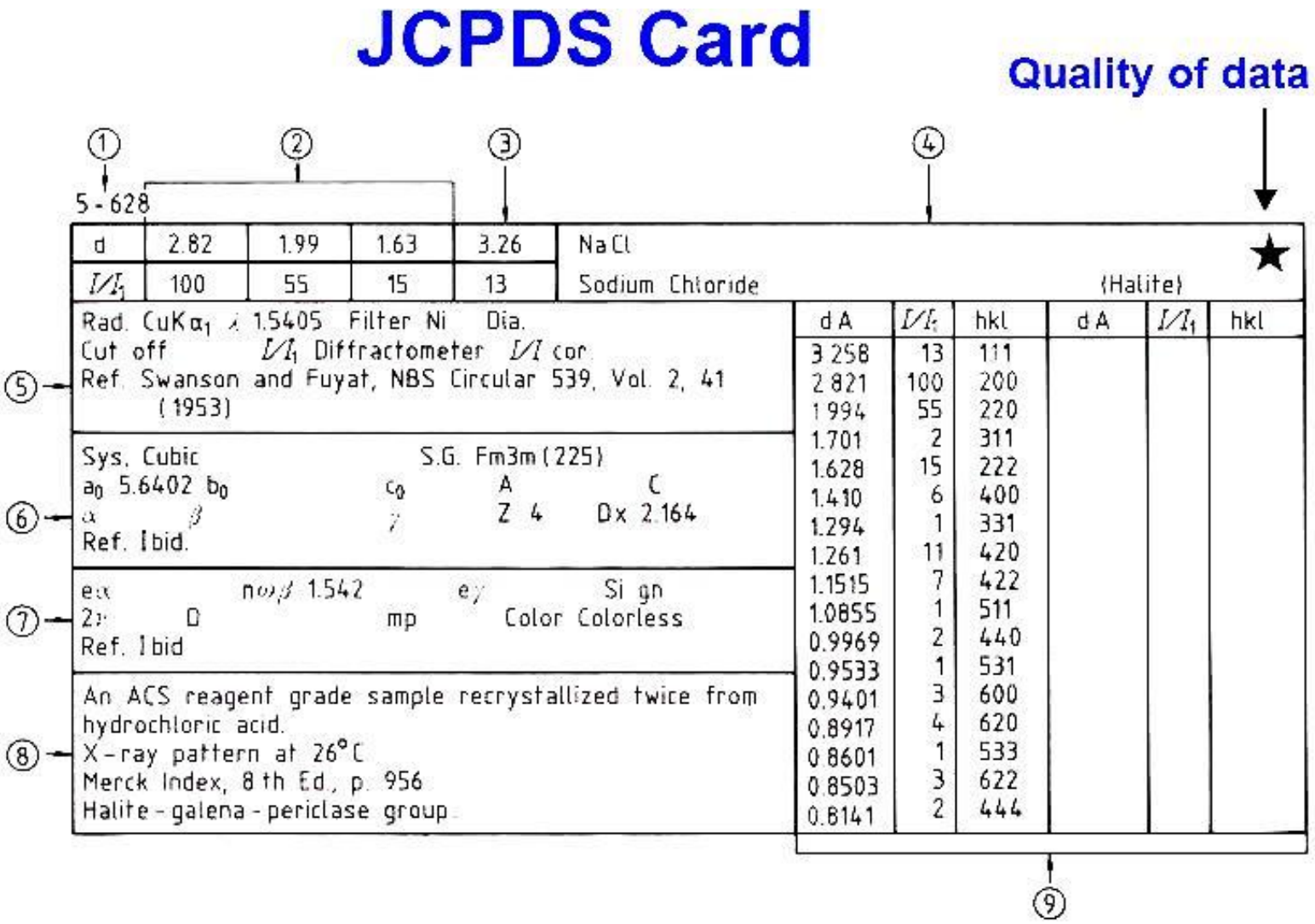

ICDD data files

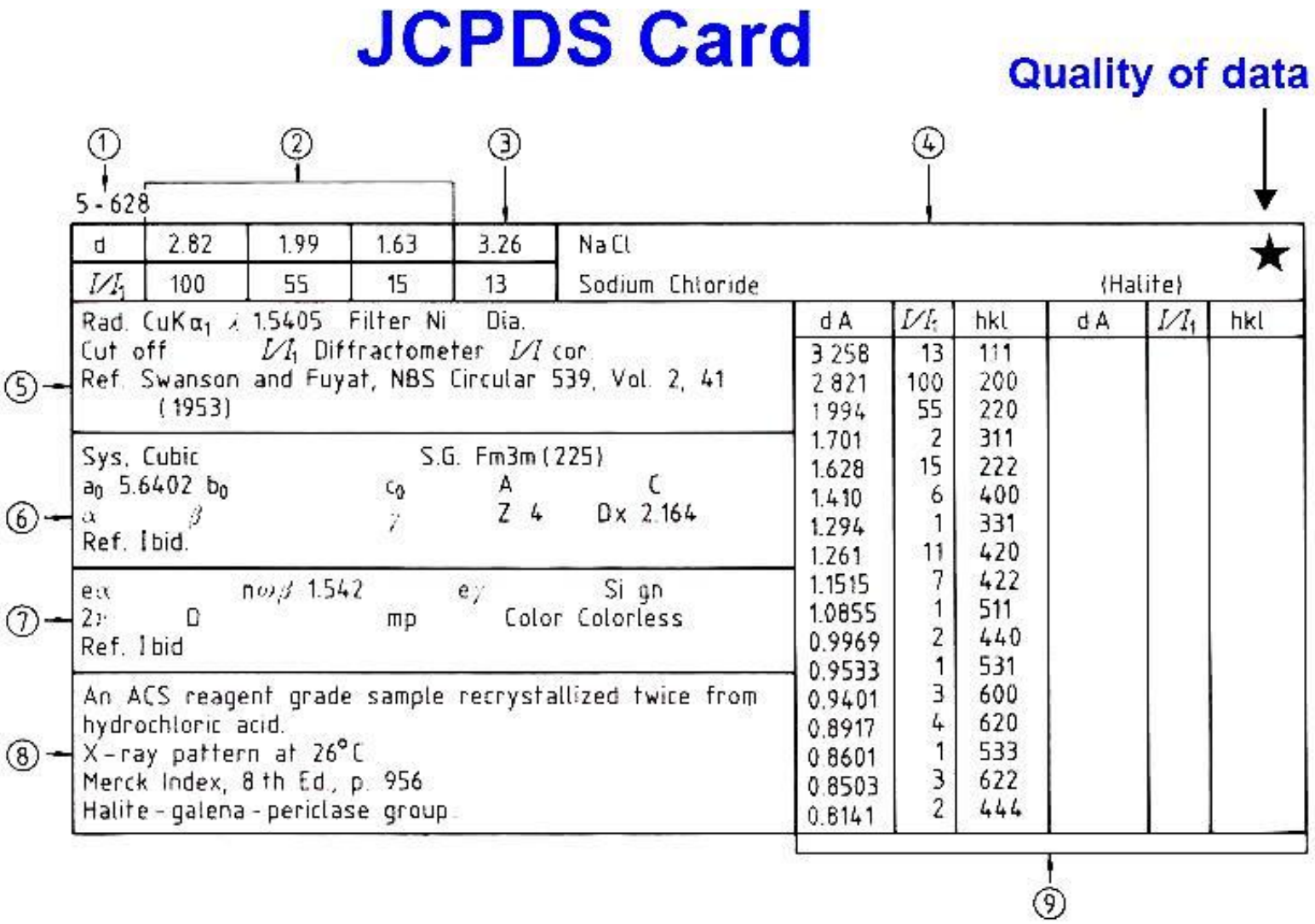

ICDD data files

4-831

Zn

Zinc

Zinc, syn

Rad. $CuK\alpha_1$ λ 1.5405 Filter Ni d-sp
Cut off Int. Diffractometer $I/I_{cor.}$ 3.80
Ref. Swanson, Tatge, *Natl. Bur. Stand. (U.S.), Circ. 539*, 1 16 (1953)

Sys. Hexagonal S.G. $P6_3/mmc$ (194)
a 2.665 b c 4.947 A C 1.8563
α β γ Z 2 mp 420°
Ref. Ibid.

D_x 7.14 D_m 7.05 SS/FOM F_{20}=55.1(.0182,20)

εα nωβ 2.58 εγ Sign 2V
Ref. Winchell, *Elements of Optical Mineralogy*, 1 (1927)

Color Bluish white
Pattern at 26 C. Sample from New Jersey Zinc Company, Sterling Hill, New Jersey, USA. Spectroscopic analysis shows faint traces of Pb, Cu, Mg, Si. Merck Index, 8th Ed., p. 1127. Zinc group. PSC: hP2.

d Å	Int	hkl	d Å	Int	hkl
2.473	53	002			
2.308	40	100			
2.091	100	101			
1.687	28	102			
1.342	25	103			
1.332	21	110			
1.237	2	004			
1.1729	23	112			
1.1538	5	200			
1.1236	17	201			
1.0901	3	104			
1.0456	5	202			
0.9454	8	203			
0.9093	6	105			
0.9064	11	114			
0.8722	5	210			
0.8589	9	211			
0.8437	2	204			
0.8245	1	006			
0.8225	9	212			

ICDD data files

Search / Match on the ICDD data file

Search

selection of "standards" with

$n \geq 3$

n : first peaks in a "standard"

Match

comparison of all d-I pairs in the unknown with the selected "standards"

Error : standard deviation in d weighted with I

ICDD data files

Caussin – Nusinovici – Beard 1988/89

- whole pattern search/match on the ICDD file
- all "standards" in the data file with at least 1 common line are considered
- Panelty : standards with lines at zero intensity position
- Premium : for standards with increasing number of common lines

Structure determination by diffraction,

powder diffraction,

systematic extinction,

indexing,

Patterson function

phase analysis,

data-bases and applications,

Rietveld analysis,

---

special applications,

stress-strain

texture determination,

line profile analysis

the Rietveld method

structure refinement from powder patterns

the principle of the Rietveld Method is

to minimize a function M, the difference between

the measured diffraction pattern y^{obs}

and the calculated pattern y^{calc}

$$M = \sum_i W_i \left\{ y_i^{obs} - \frac{1}{c} y_i^{calc} \right\}^2$$

W_i : weights, c : scaling factor

Analytical Line-Profile Functions

Lorentzian [L]:

$$I(x) = I_0 \frac{w^2}{w^2 + x^2}$$

where FWHM = $2w$

Gaussian [G]:

$$I(x) = I_0 \exp(-\pi x^2 / \beta^2)$$

where $w = \beta [\ln 2 / \pi]^{1/2}$

the Rietveld method

Pearson VII [PVII]:

$$I(x) = I_o \left(\frac{1}{1 + cx^2} \right)^m$$

where m is Pearson VII index and $c = f(w) = (2^{1/m} - 1)/w^2$

([PVII] → [G] as $m \to \infty$)

Pseudo-Voigtian [Ps-Vt]:

$$I(x) = I_o \{ \eta [L] + (1-\eta)[G] \}$$

where η is the Lorentzian fraction or Ps-Vt mixing factor

Voigtian [V]:

Convolution of [L] and [G] functions, or

$$[V] = [L] * [G]$$

the Rietveld method

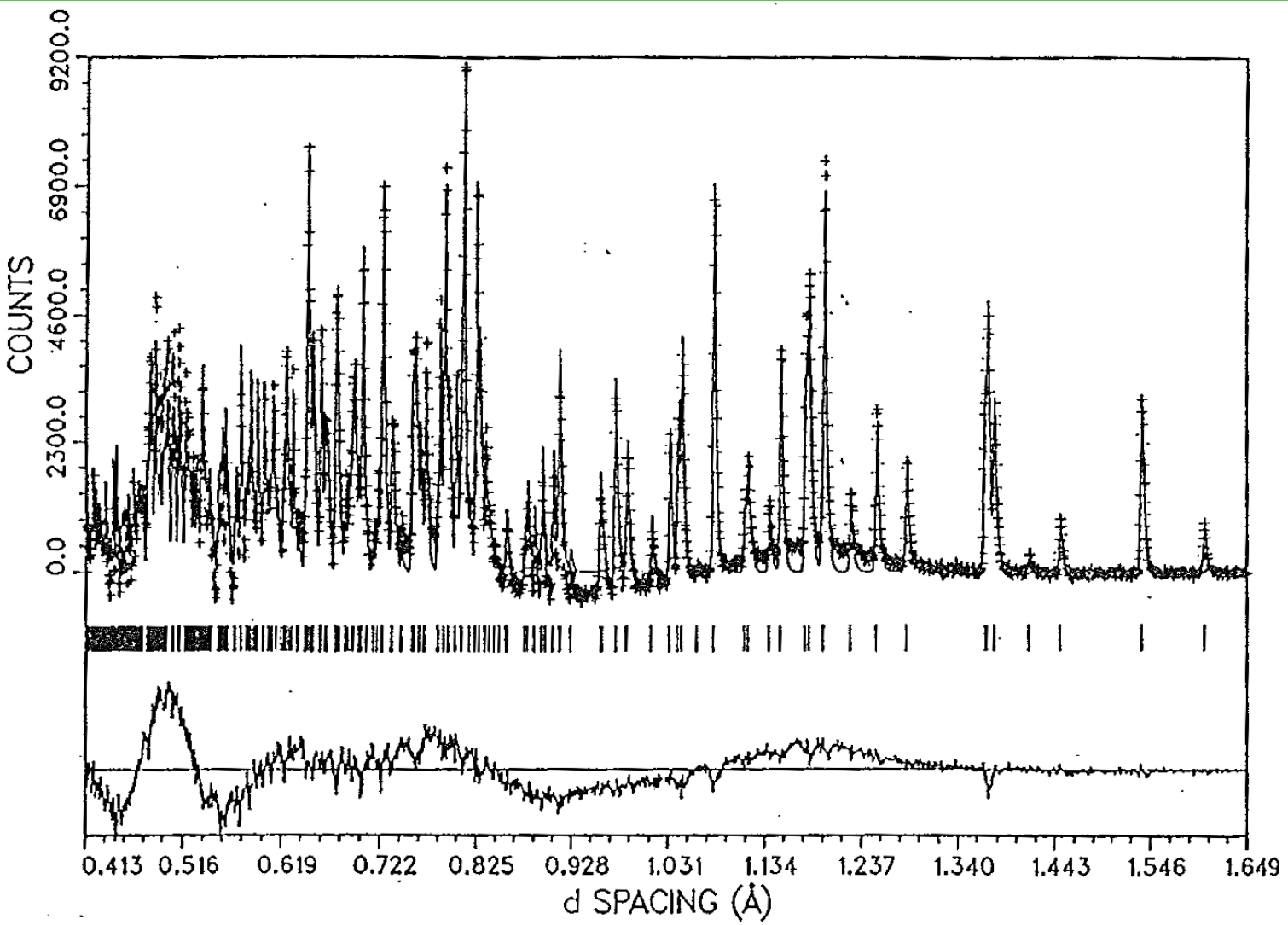

Fig. 6.5 Rietveld profile fit for a 50:50 mixture of crystalline quartz and amorphous silica, before Fourier-filtering. See Fig. 6.1 for explanation of symbols.

香港城市大學
City University of Hong Kong

R.A.Jung: The Rietveld Method, 1993

Structure determination by diffraction,

powder diffraction,

systematic extinction,

indexing,

Patterson function

phase analysis,

data-bases and applications,

Rietveld analysis,

special applications,

stress-strain

---

texture determination,

line profile analysis

Macherauch, E. (~1965)
schematic classification of internal stresses

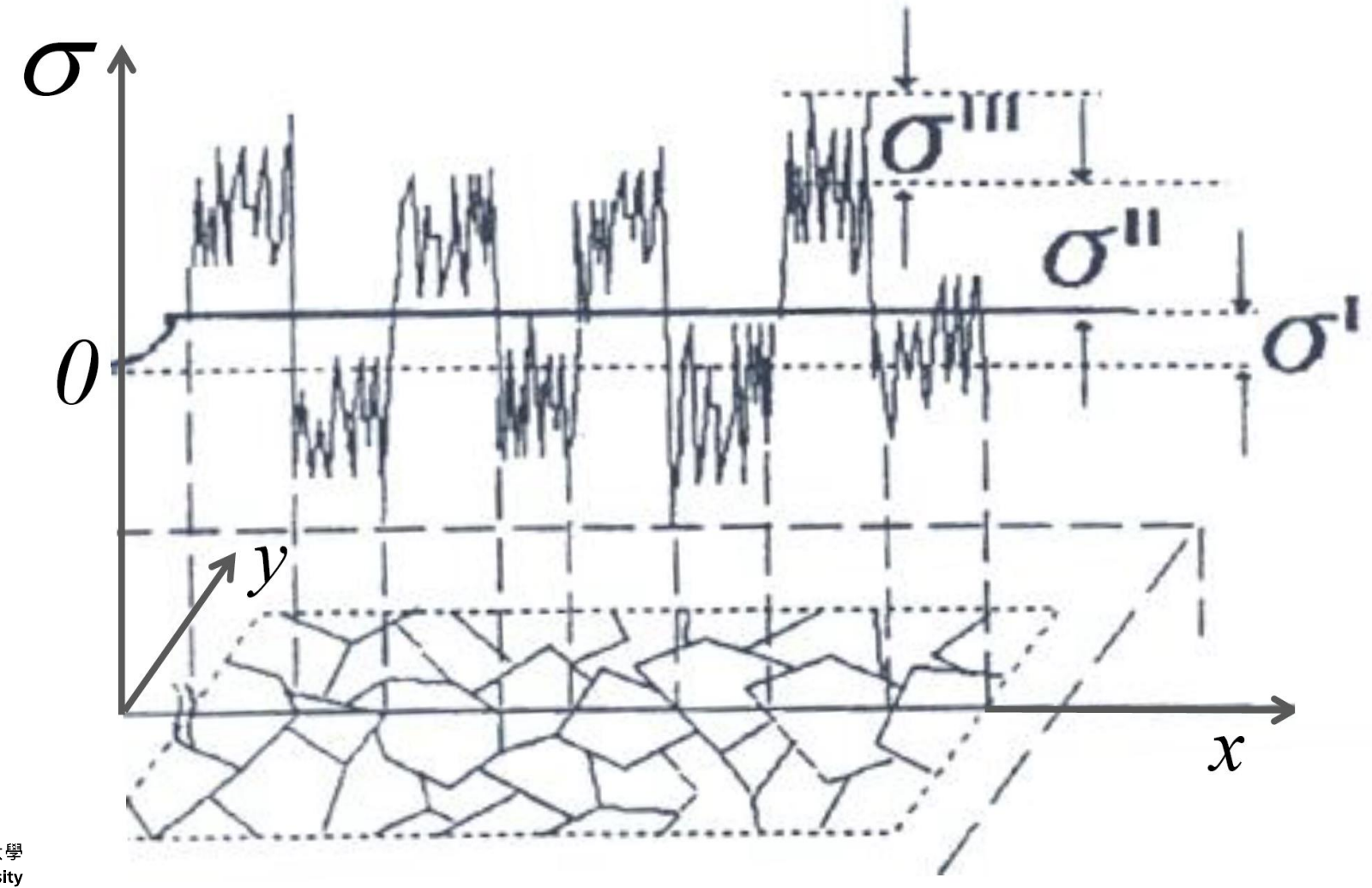

Macherauch, E. (~1965)
schematic classification of internal stresses

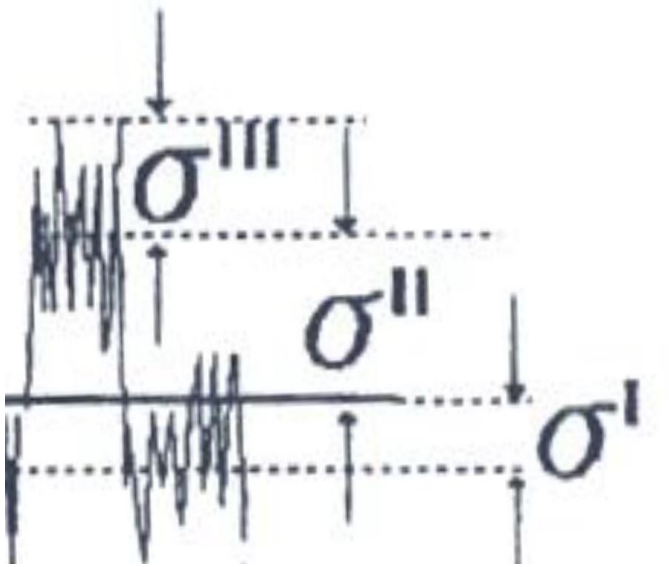

σ_I: ***macro-stress***
averaged over many grains

σ_{II}: ***intergranular-stresses***
averaged over individual grains

σ_{III}: ***micro-strains*** (or ***stresses***)
produced by ***dislocations***

stress – strain

ONLY strain can be measured

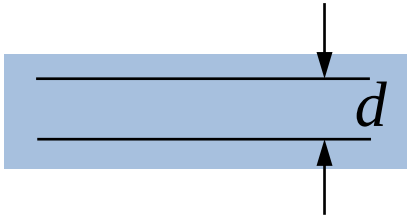

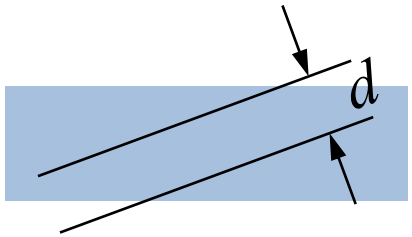

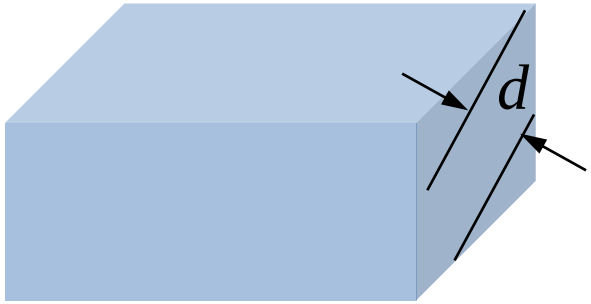

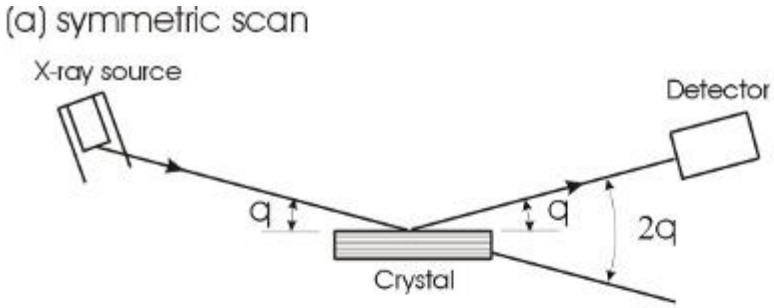

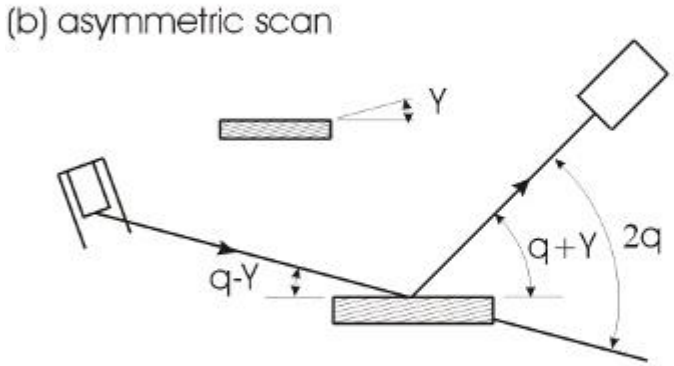

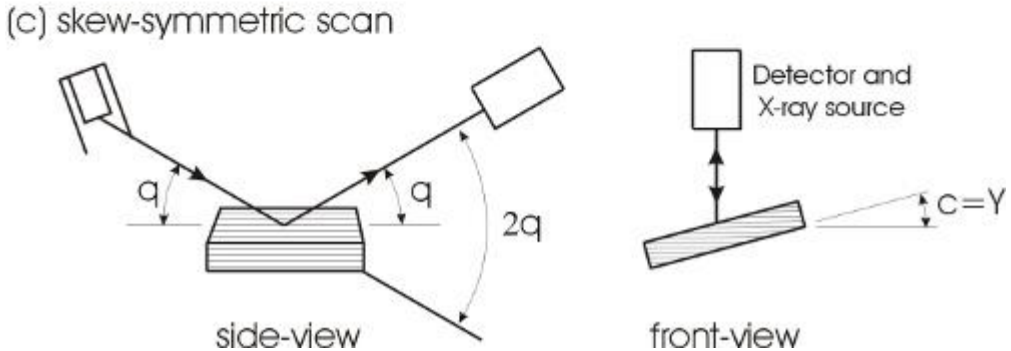

香港城市大學
City University
of Hong Kong

stress – strain

ONLY strain can be measured

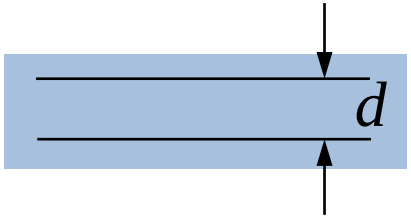

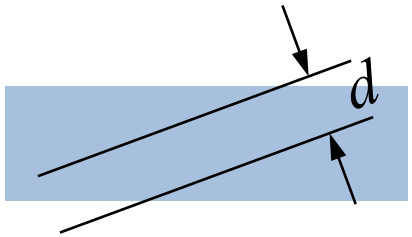

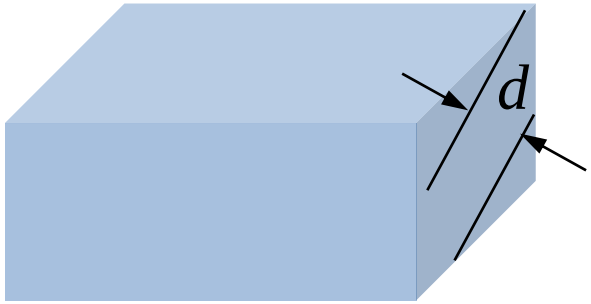

d is always measured parallel to **g**
where d is the distance of the planes normal to the **g** vector

tilting the specimen allows to determine different components of the strain-tensor

stress – strain

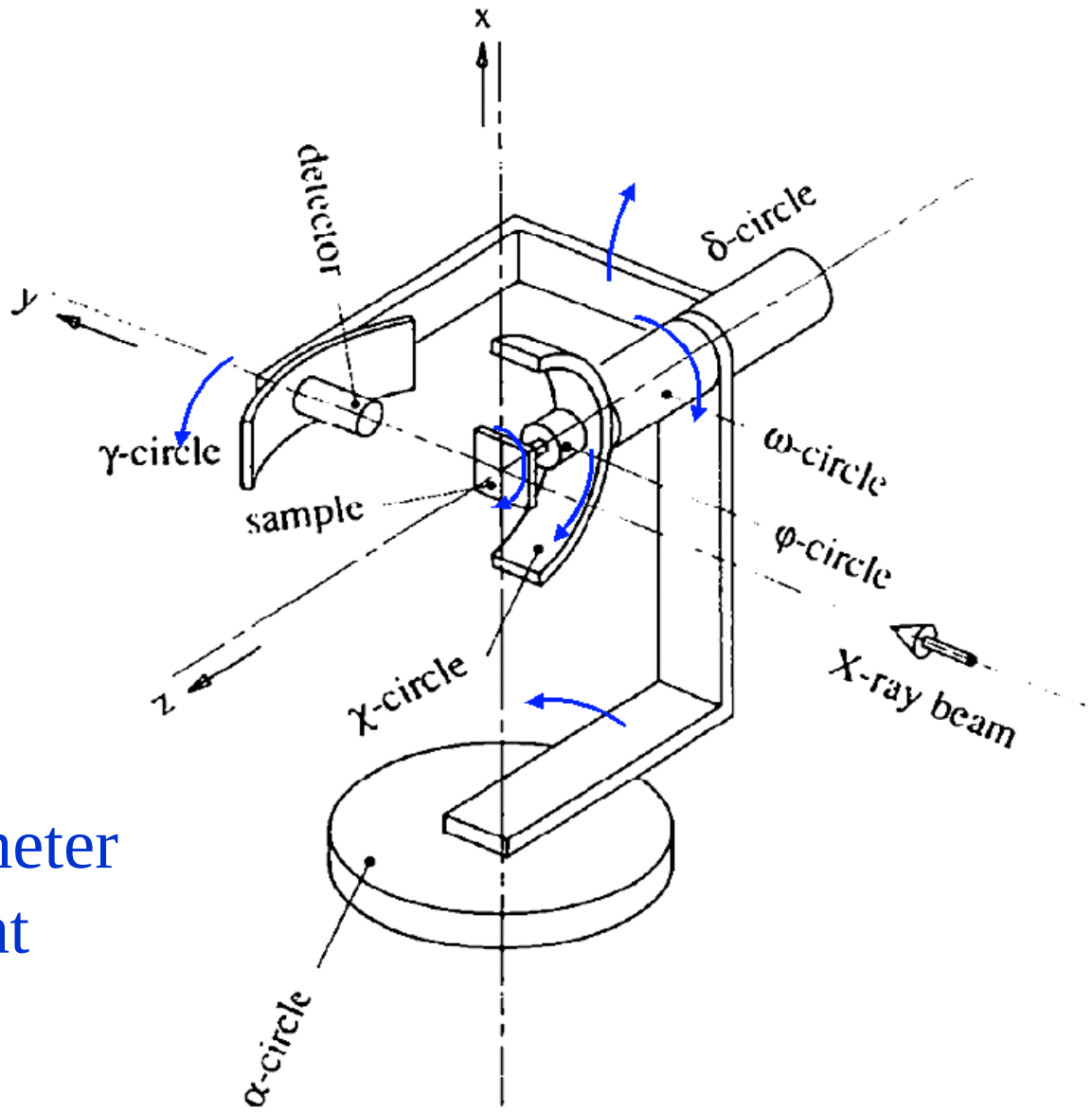

the 6-circle diffractometer
for stress measurement
at synchrotrons

香港城市大學
City University
of Hong Kong

http://www.opengda.org/documentation/manuals/Diffcalc/trunk/user/manual.html

stress – strain

usual notations for X-ray
stress-strain experiments

S_1, S_2, S_3 : sample coordinates
L_1, L_2, L_3 : laboratory coordinates

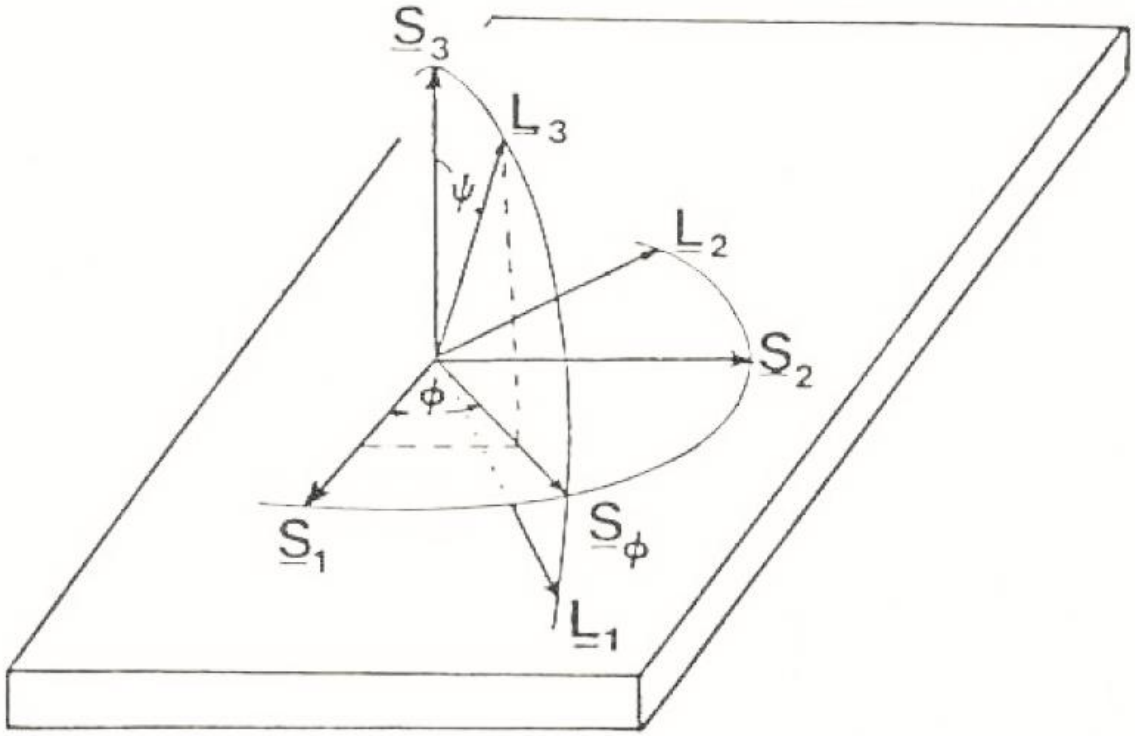

stress – strain

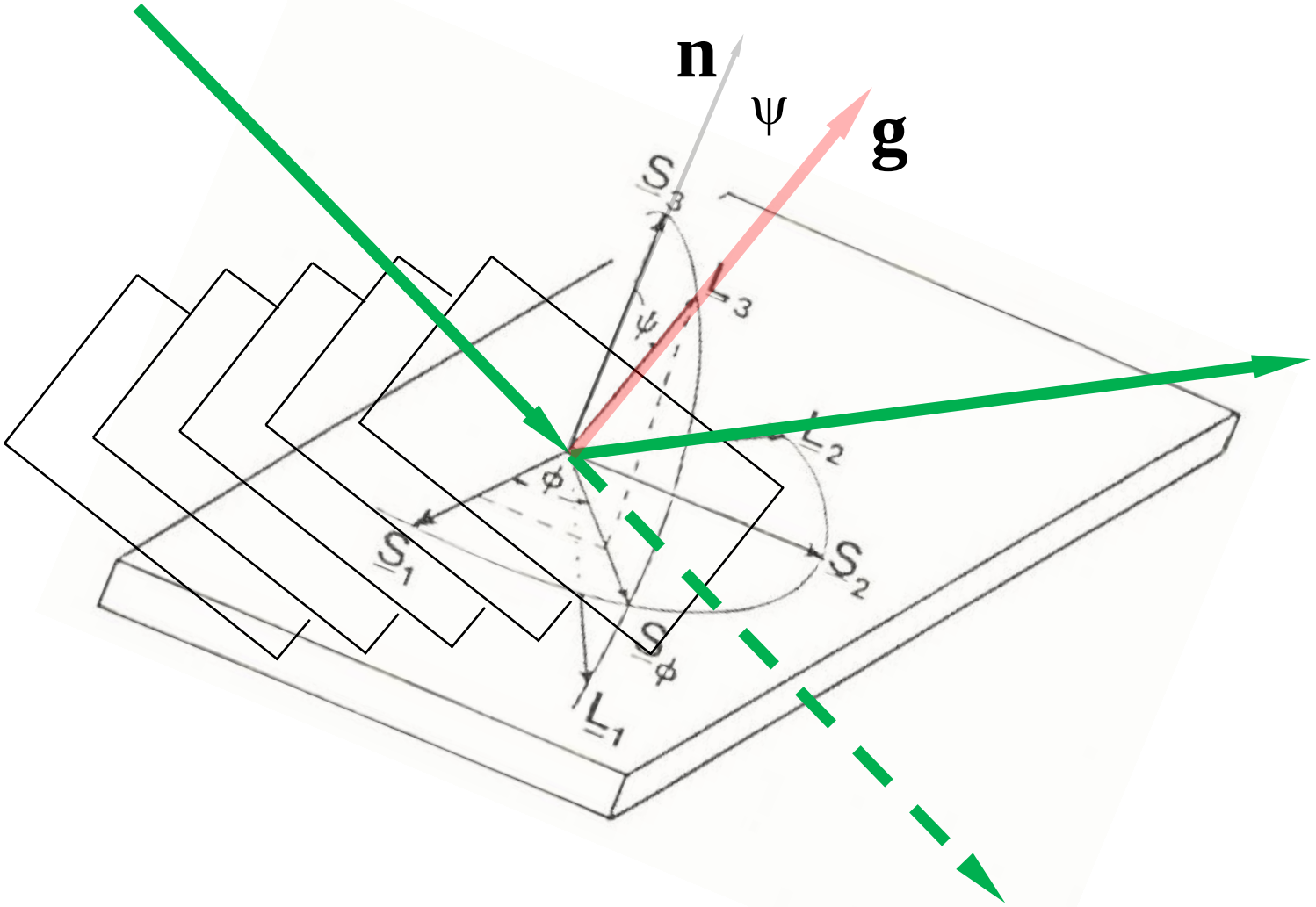

stress – strain

$$(\varepsilon'_{33})_{\phi\psi} = \frac{d_{\phi\psi} - d_0}{d_0} = \varepsilon_{11}\cos^2\phi\sin^2\psi + \varepsilon_{12}\sin 2\phi\sin^2\psi + \varepsilon_{22}\sin^2\phi\sin^2\psi$$
$$+ \varepsilon_{33}\cos^2\psi + \varepsilon_{13}\cos\phi\sin 2\psi + \varepsilon_{23}\sin\phi\sin 2\psi \qquad (1)$$

sample coordinates

laboratory coordinates

stress – strain

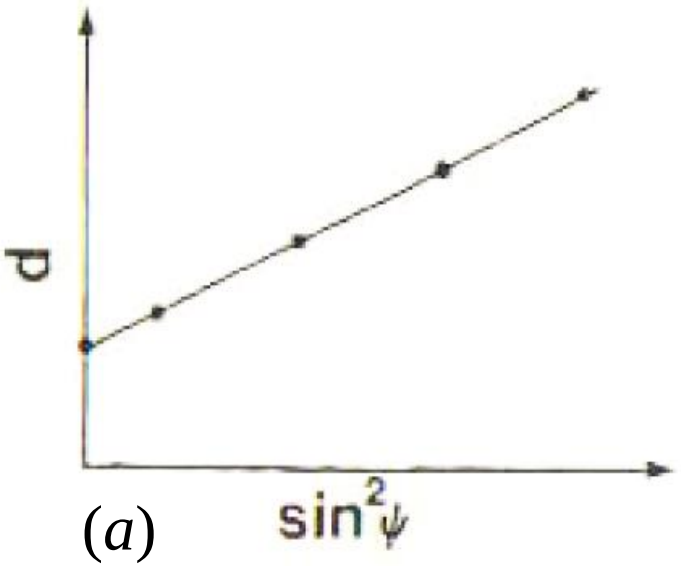

(*a*)

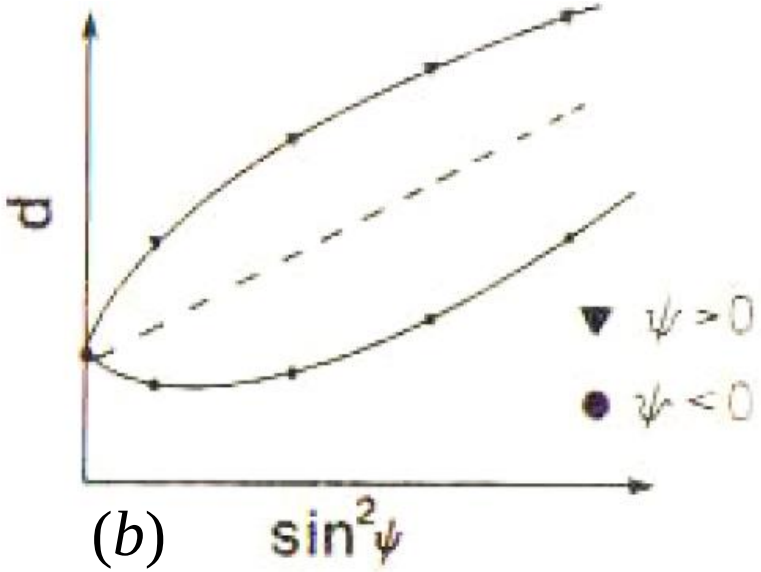

(*b*)

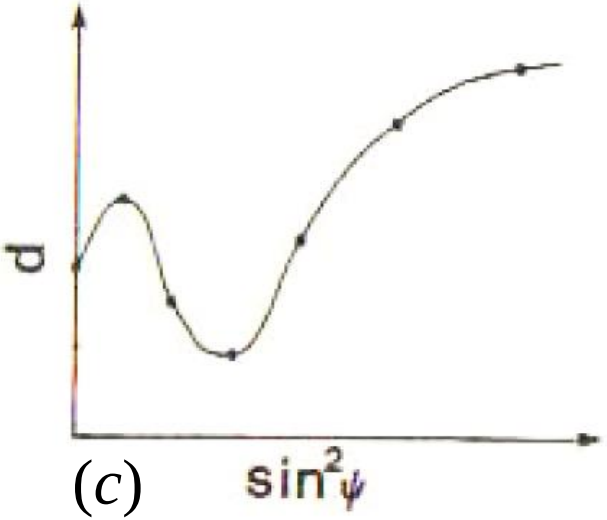

(*c*)

typical plots

a, *b* : eq. (1) can be solved

c : eq. (1) cannot be solved

lattice – strains

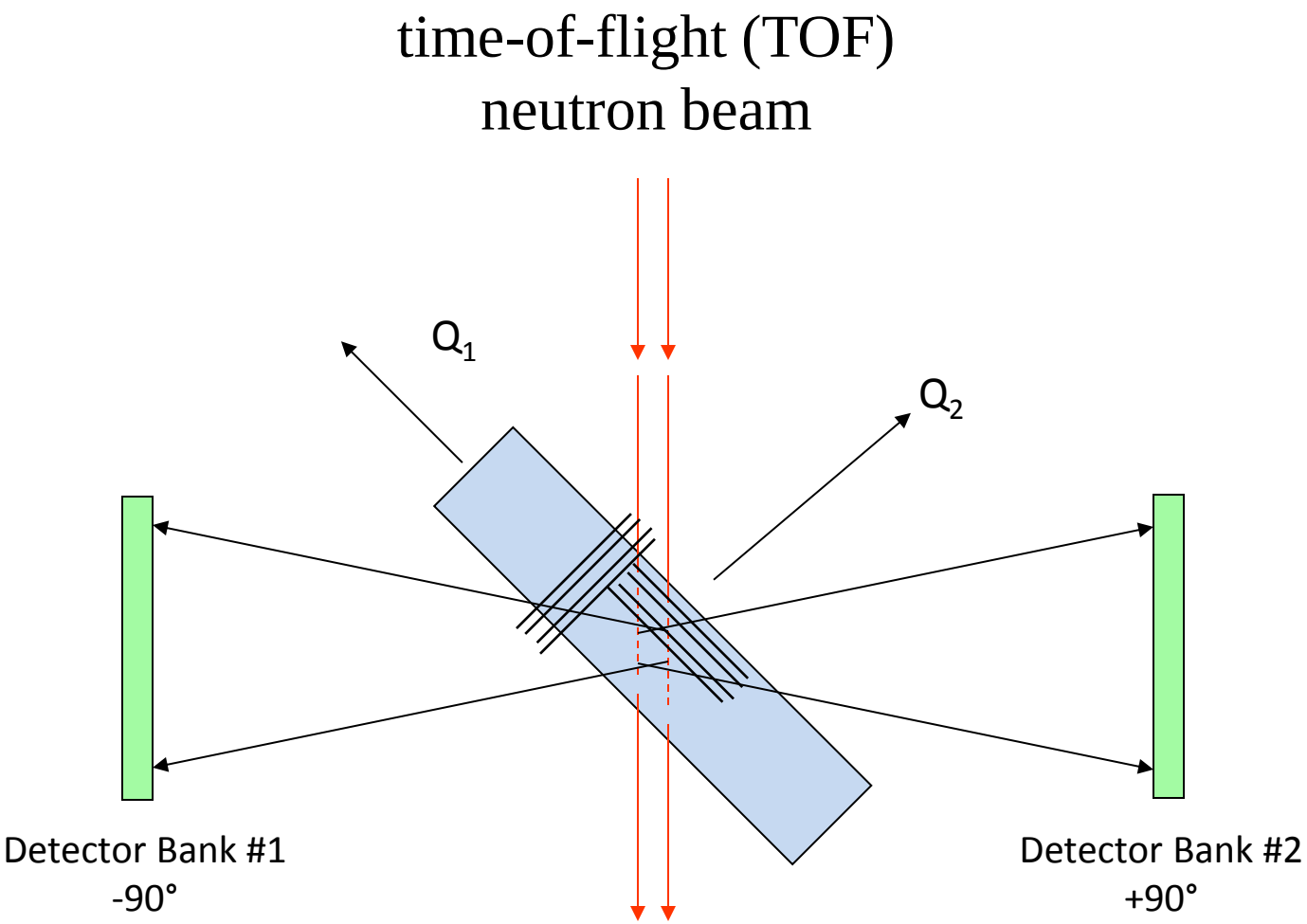

lattice – strains

Detector Banks + Collimators VULCAN, SNS, Oak Ridge

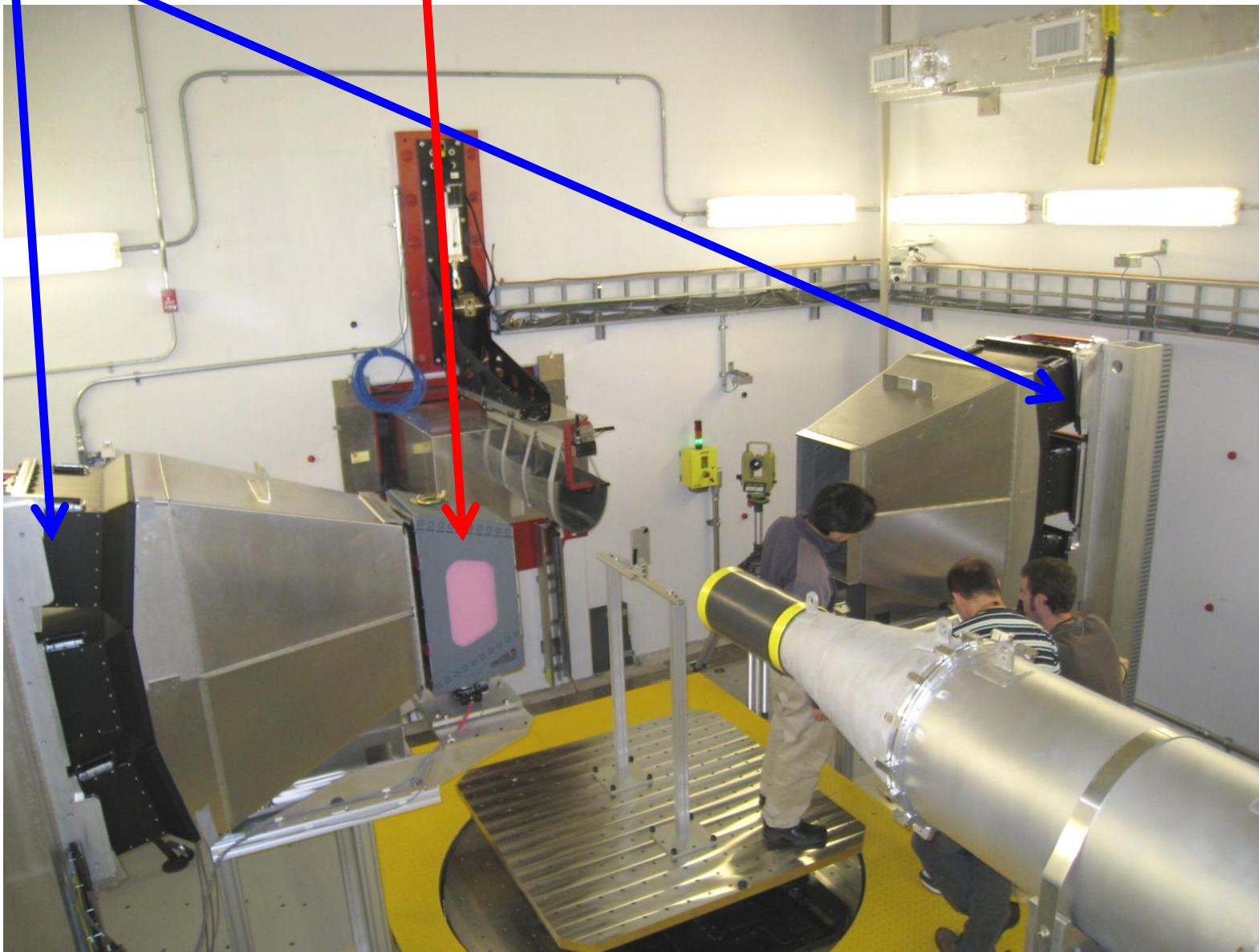

lattice – strains

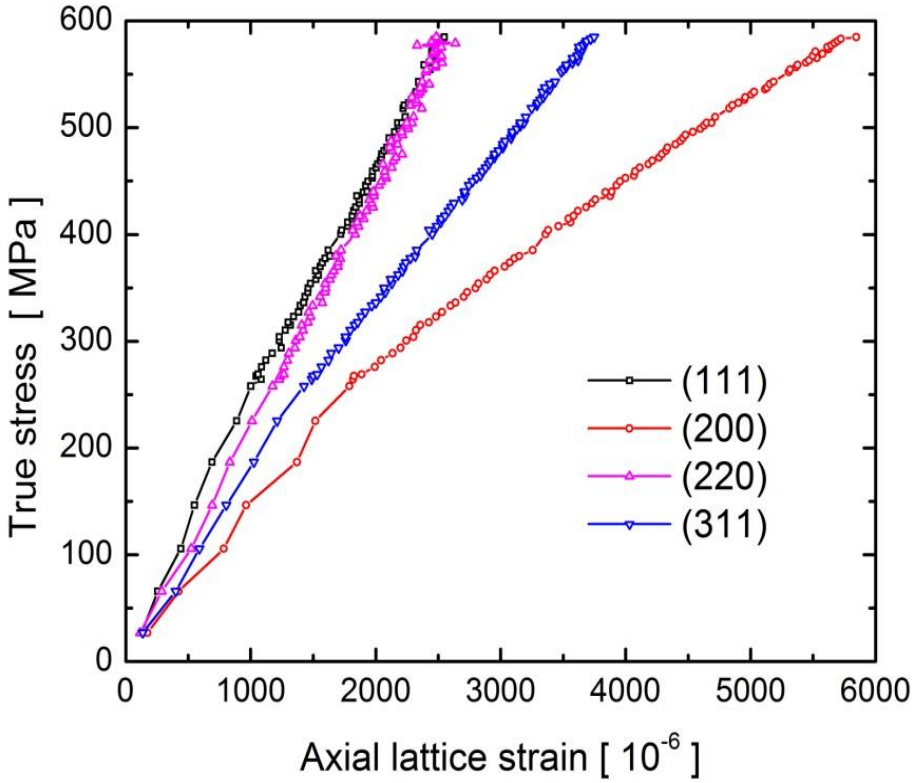

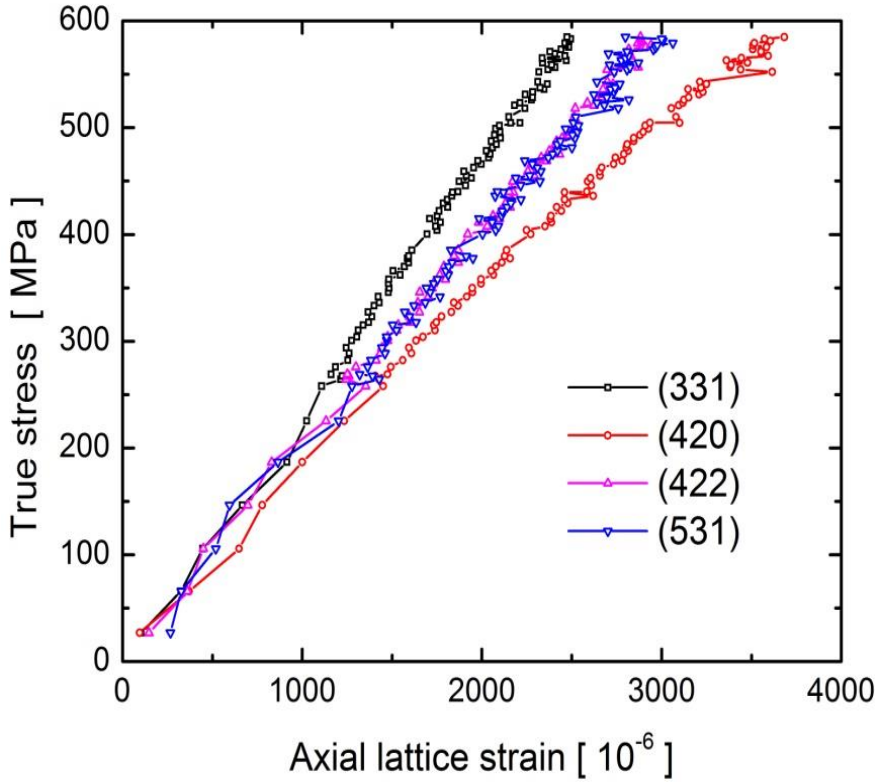

316 stainless-steel

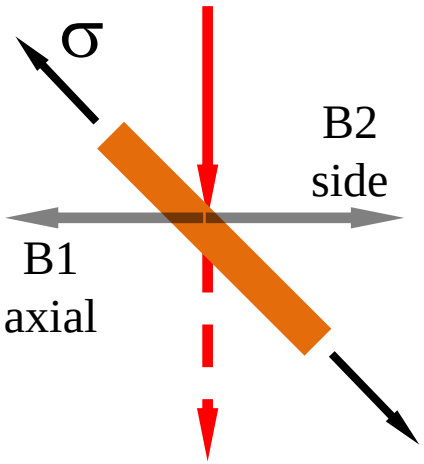

香港城市大學
City University
of Hong Kong

Structure determination by diffraction,

powder diffraction,

systematic extinction,

indexing,

Patterson function

phase analysis,

data-bases and applications,

Rietveld analysis,

special applications,

stress-strain

texture determination,

---

line profile analysis

texture

bulk, polycrystalline materials
consist almost
NEVER
of randomly oriented
grains or crystallites

the distribution of the
crystallographic orientation of
grains or crystallites is
TEXTURE

texture

random

preferred orientation

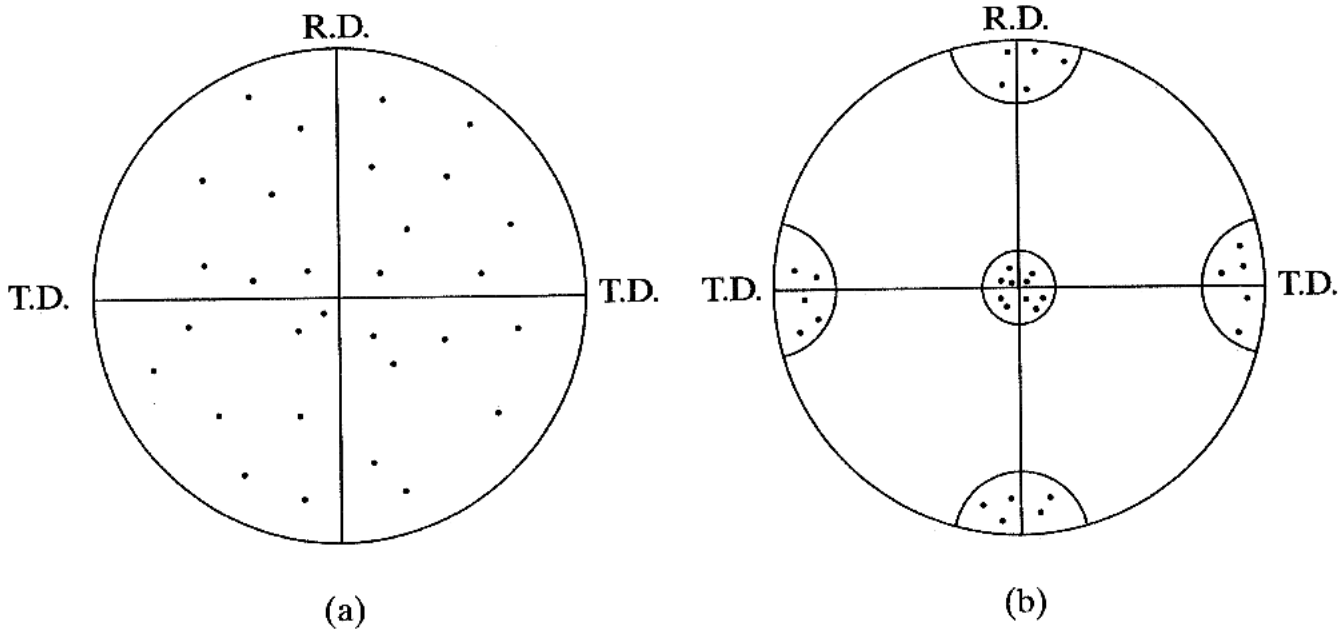

Figure 14-9 (100) pole figures for sheet material, illustrating (a) random orientation and (b) preferred orientation. R.D. (rolling direction) and T.D. (transverse direction) are reference directions in the plane of the sheet.

B.D.Cullity & S.R.Stock, Elements of X-ray Diffraction

texture

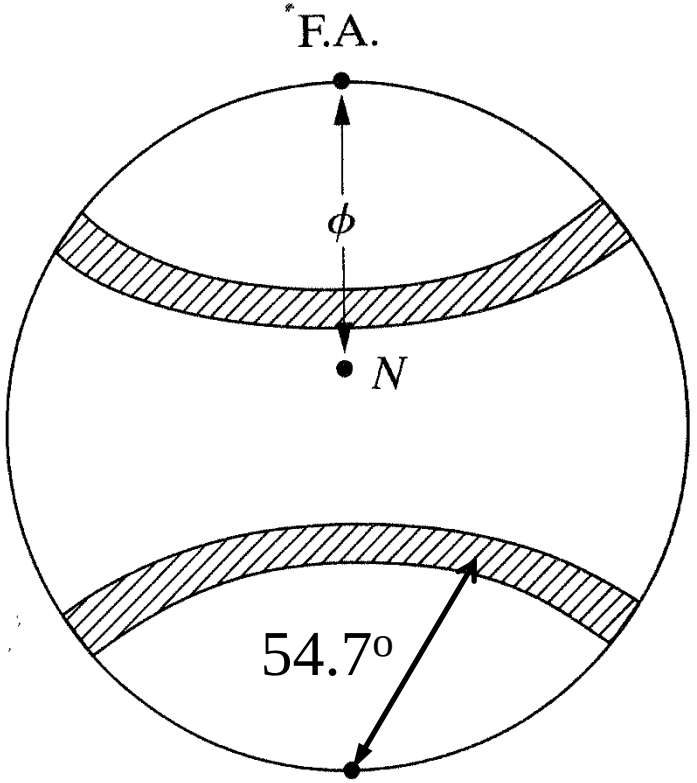

Figure 14-10 (111) pole figure for an imperfect [100] fiber texture. F.A. = fiber axis. Cross-hatched areas are areas of high (111) pole density.

B.D.Cullity & S.R.Stock, Elements of X-ray Diffraction

texture

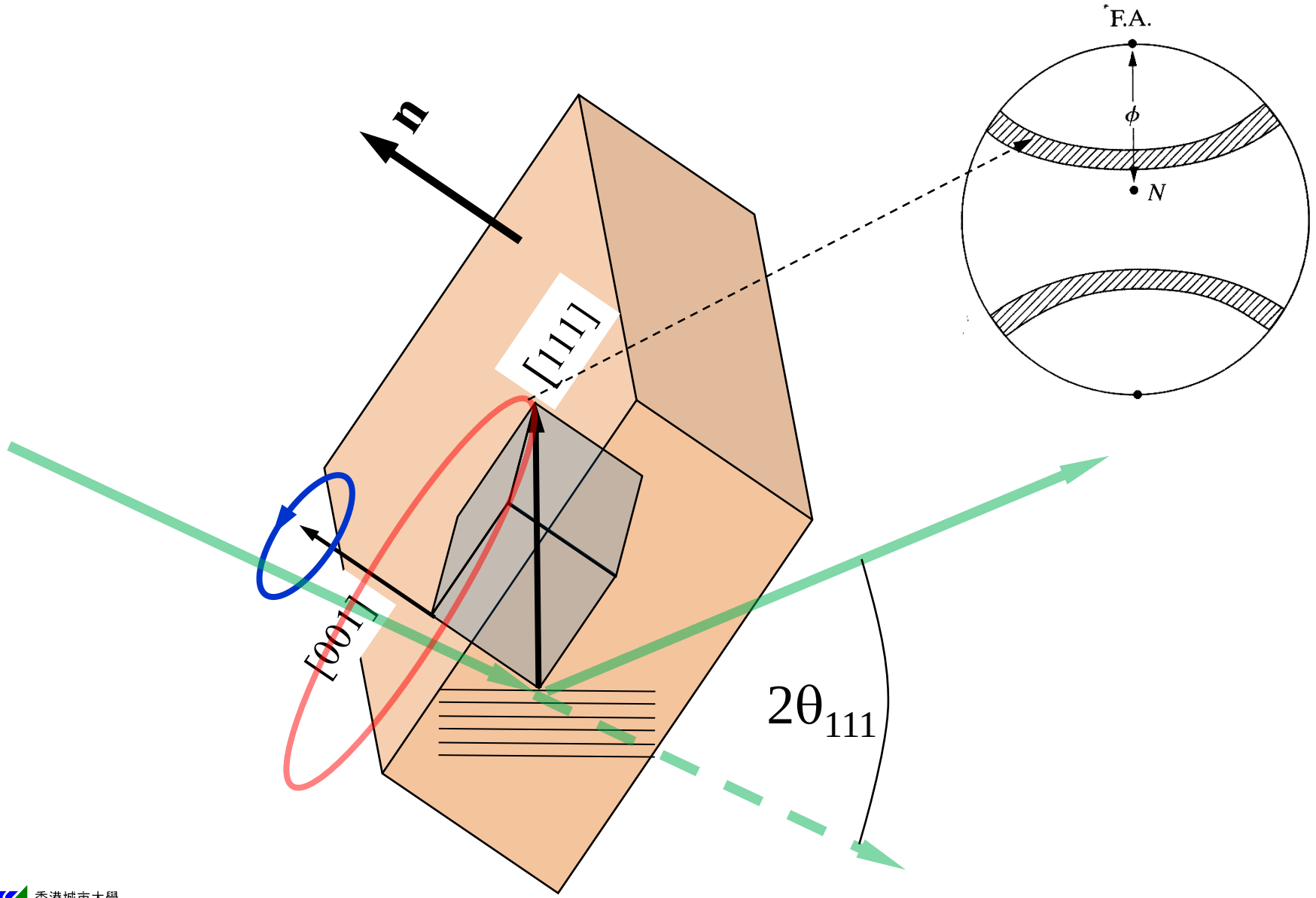

texture

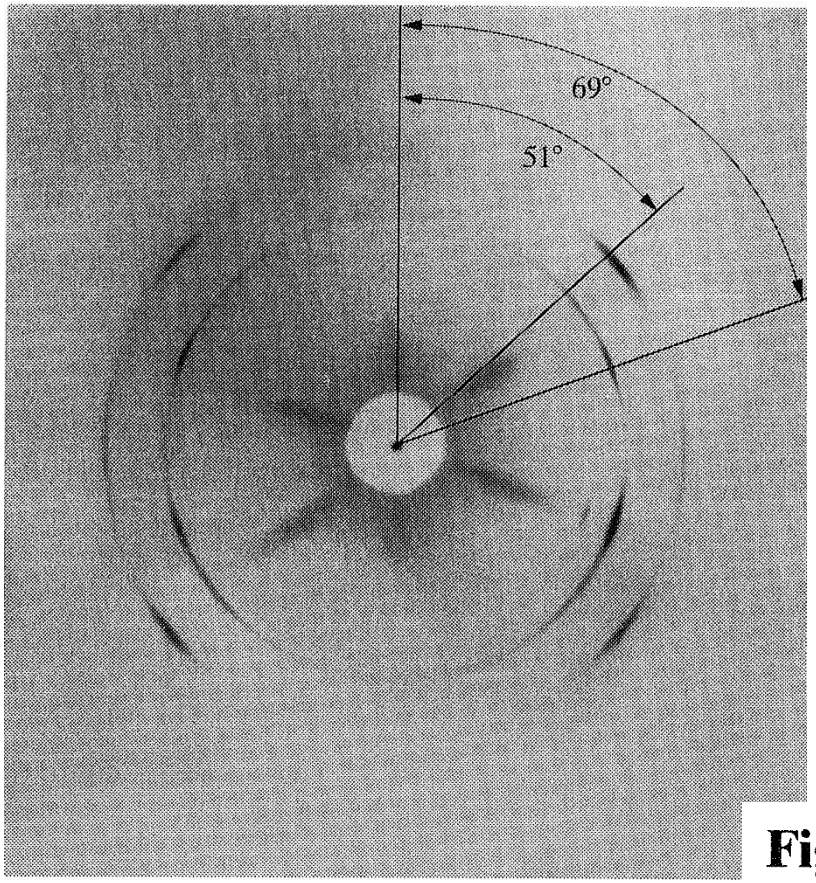

Figure 14-13 Transmission pinhole pattern of cold-drawn aluminum wire, wire axis vertical. Filtered copper radiation. (The radial streaks near the center are formed by the white radiation in the incident beam.)

B.D.Cullity & S.R.Stock, Elements of X-ray Diffraction

texture

Figure 14-14 Transmission method for pole-figure determination. After Geisler [14.15].

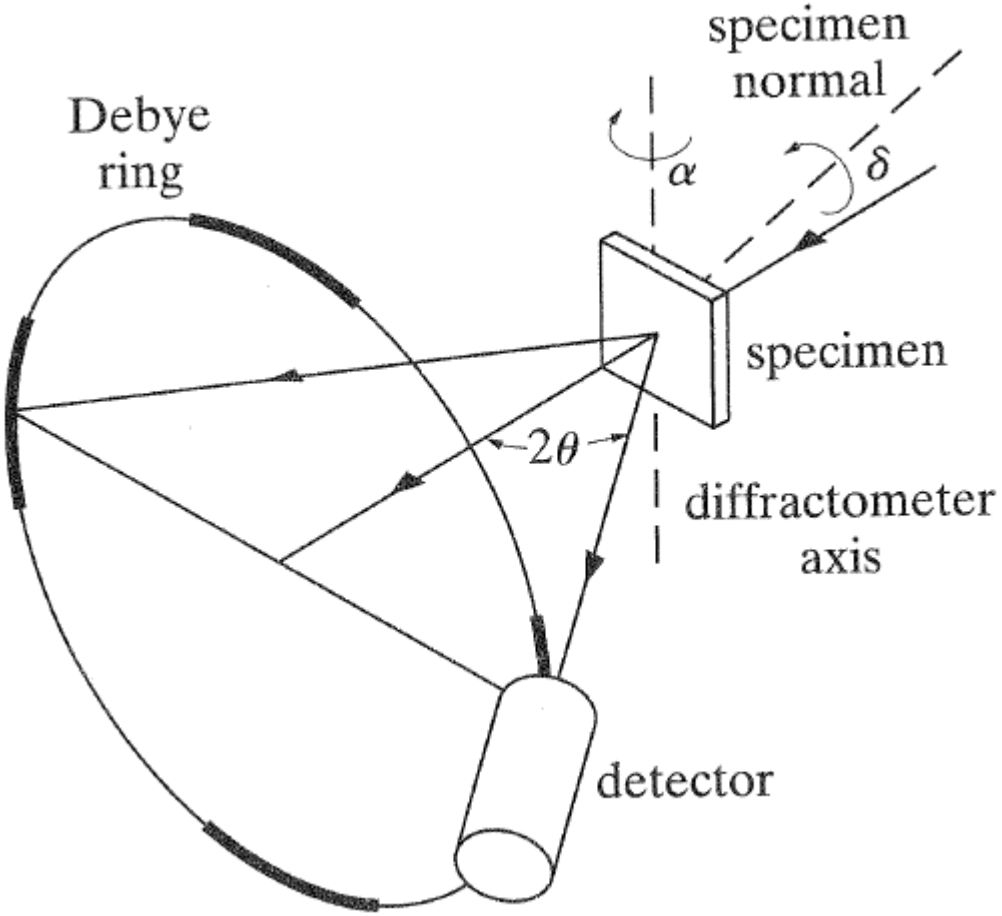

specimen is rotated over two axes

B.D.Cullity & S.R.Stock, Elements of X-ray Diffraction

texture

brass-texture

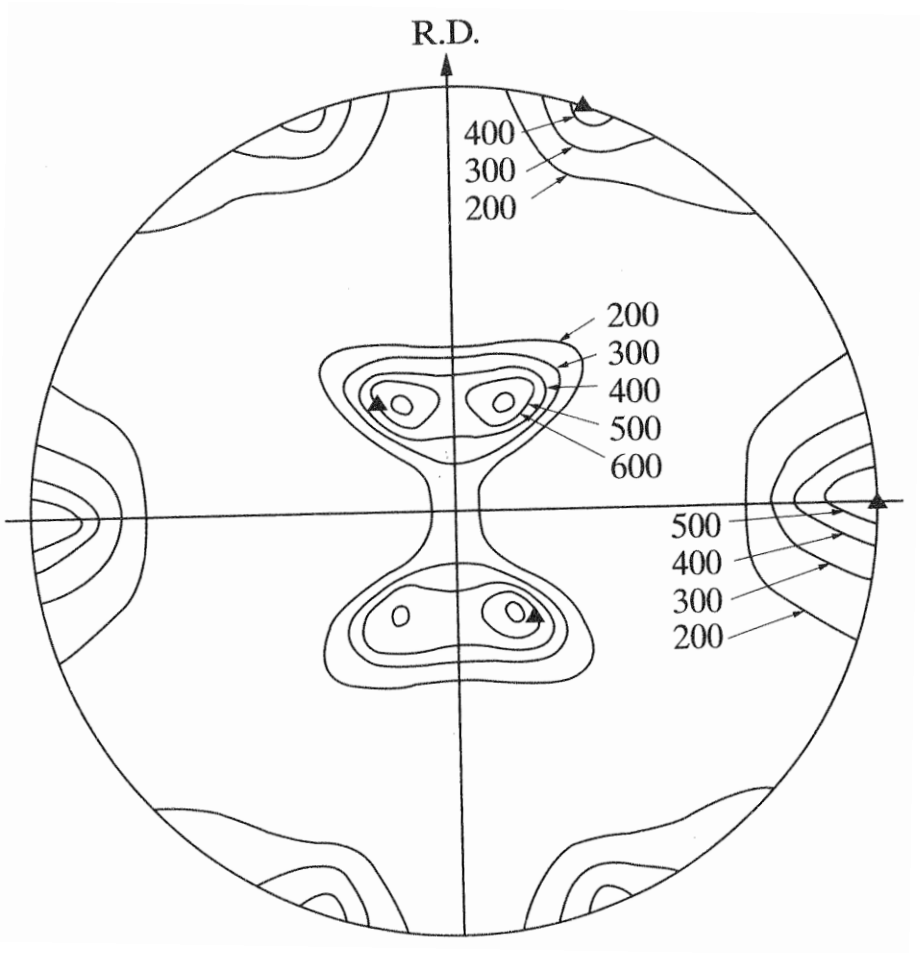

Figure 14-21 (111) pole figure of alpha brass sheet (70 Cu-30 Zn), cold rolled to a reduction in thickness of 95 percent. Pole densities in arbitrary units. The outer parts of all four quadrants were determined experimentally; the inner parts of the upper right and lower left quadrants were measured, and the other two constructed by reflection. The solid triangles show the (110) [112] orientation. Hu, Sperry, and Beck [14.24].

B.D.Cullity & S.R.Stock, Elements of X-ray Diffraction

texture

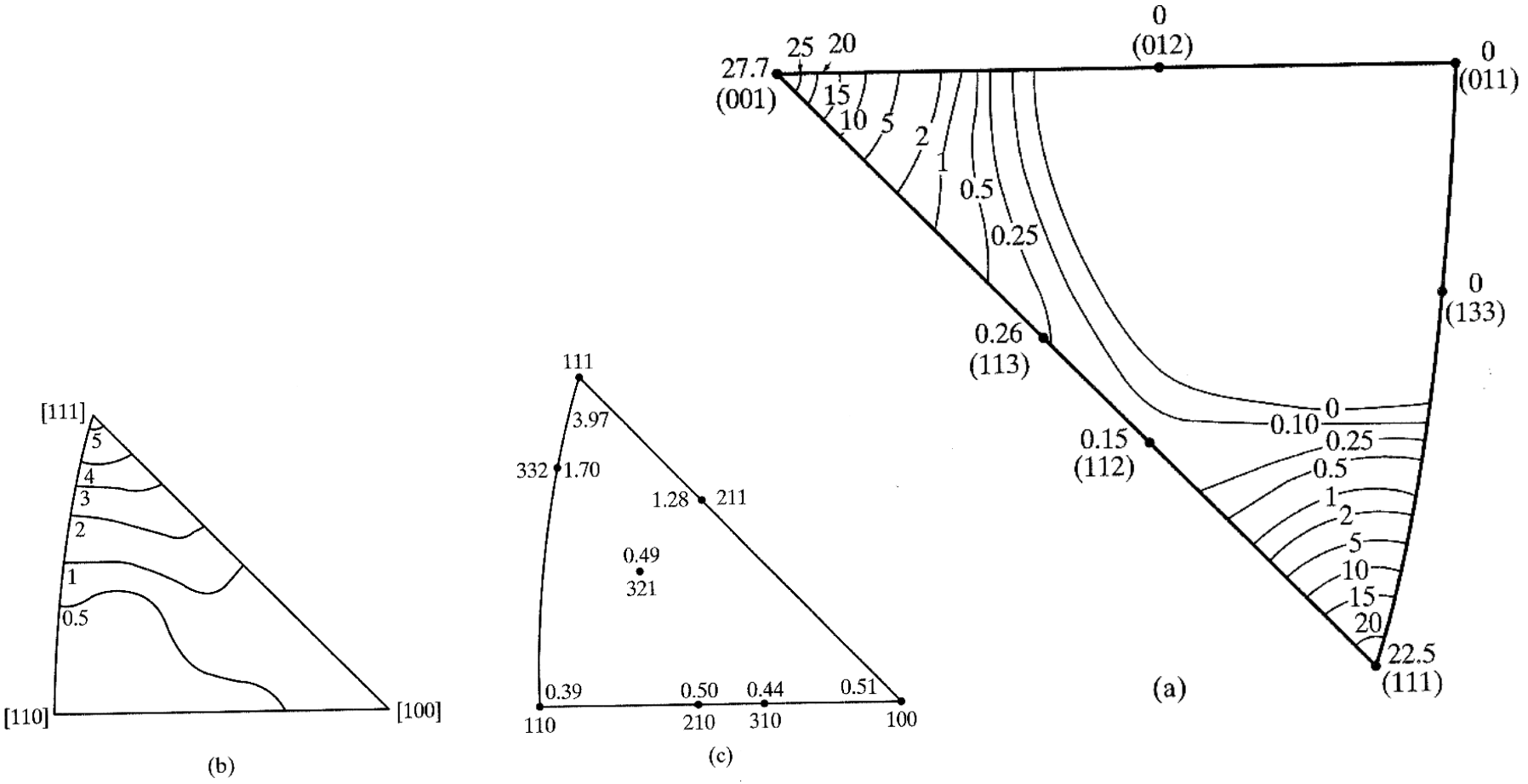

Figure 14-26 Inverse pole figures. (a) Distribution of axis of aluminum rod, extruded at 450°F to a reduction in area of 92 percent and a final diameter of 23 mm. Jetter, McHargue, and Williams [14.31]. (b) and (c) show the distribution of the sheet normal for the steel sheet of Fig. 14.22. Bunge and Roberts [14.26].

texture

orientation-distribution-function (ODF)

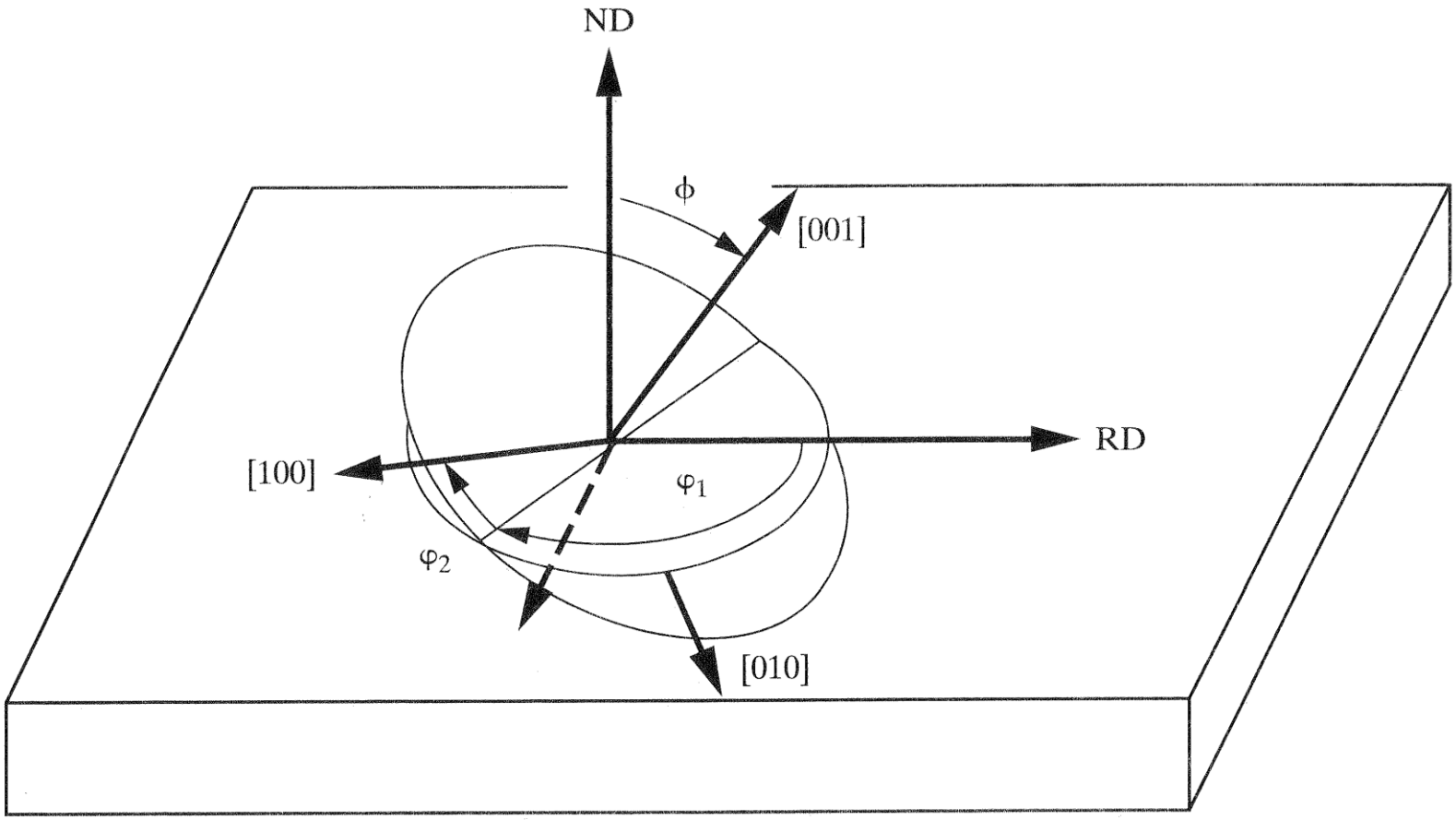

B.D.Cullity & S.R.Stock, Elements of X-ray Diffraction

texture

ODF
cold-rolled brass

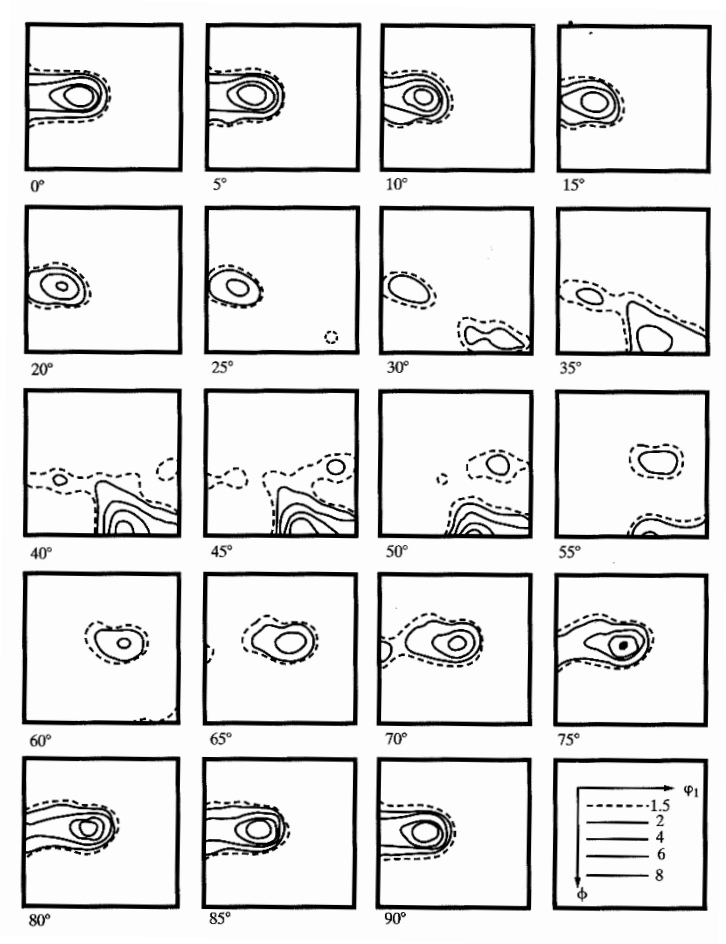

Figure 14-28 Orientation distribution function for brass cold-rolled 95%. Planes of constant φ_2 spaced every 5° are shown. The contours of equal density (times random) and orientations of φ_1 and ϕ are shown at the lower right. [14.41].

Structure determination by diffraction,

powder diffraction,

- systematic extinction,
- indexing,
- Patterson function

phase analysis,

data-bases and applications,

Rietveld analysis,

special applications,

- stress-strain
- texture determination,
- line profile analysis

Macherauch, E. (~1965)
schematic classification of internal stresses

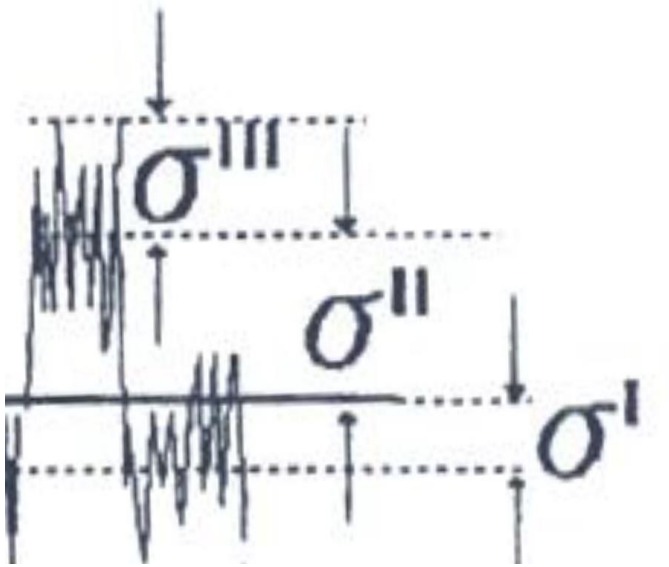

σ_I: ***macro-stress***
averaged over many grains

σ_{II}: ***intergranular-stresses***
averaged over individual grains

σ_{III}: ***micro-strains*** (or ***stresses***)
produced by ***dislocations***

+ *other effects*

Line broadening is **small**

Ni ball-milled for 12 hours

P. Scardi M. Leoni, *Acta Cryst*. (2002). A**58**, 190-200

Logarithmic intensity scale

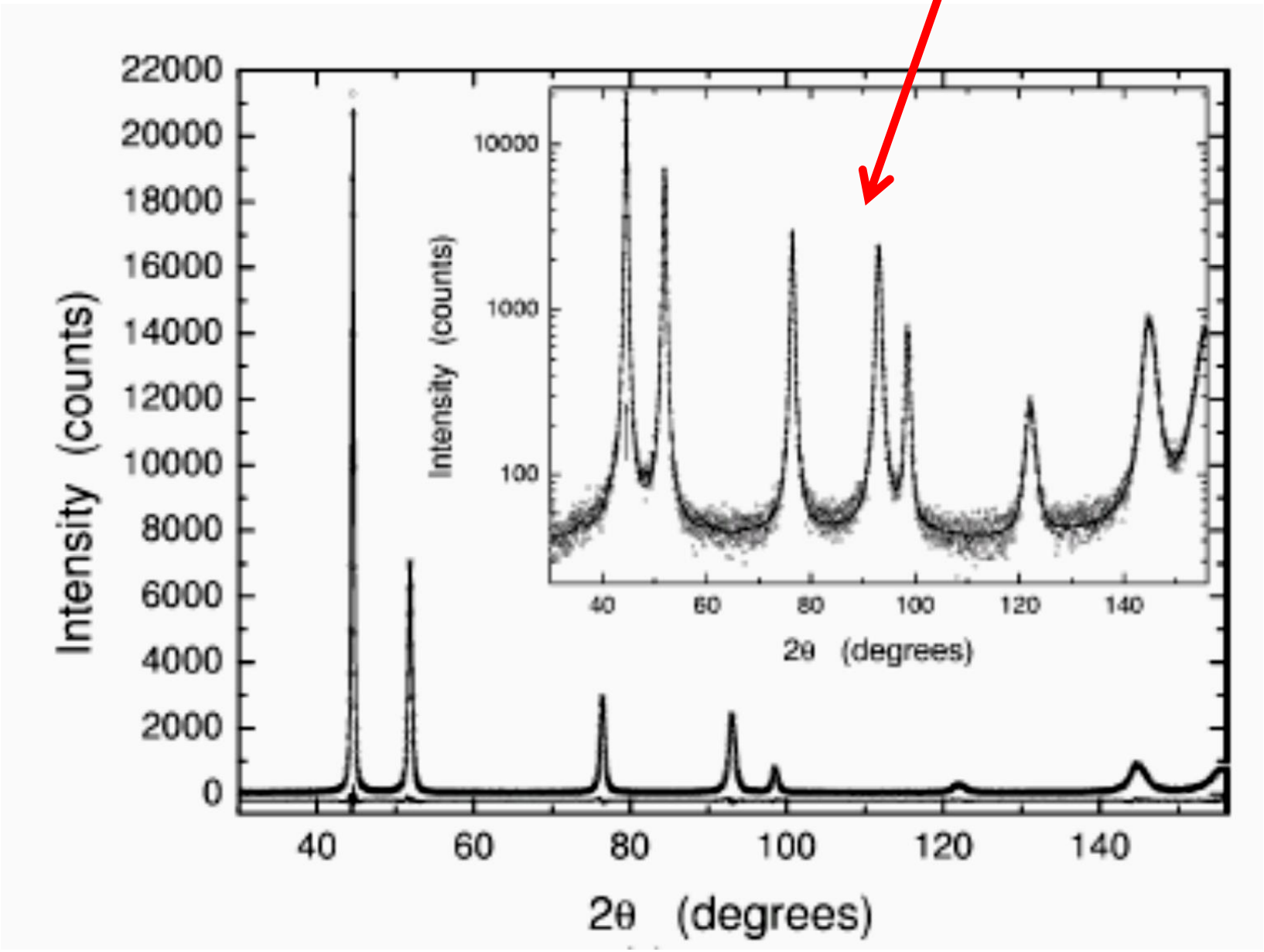

Al-3 wt% Mg ball-milled for **6 hours**

G. Ribárik, J. Gubicza, T. Ungár, *Mater. Sci. Eng. A*, 387-389 (2004) 343-347.

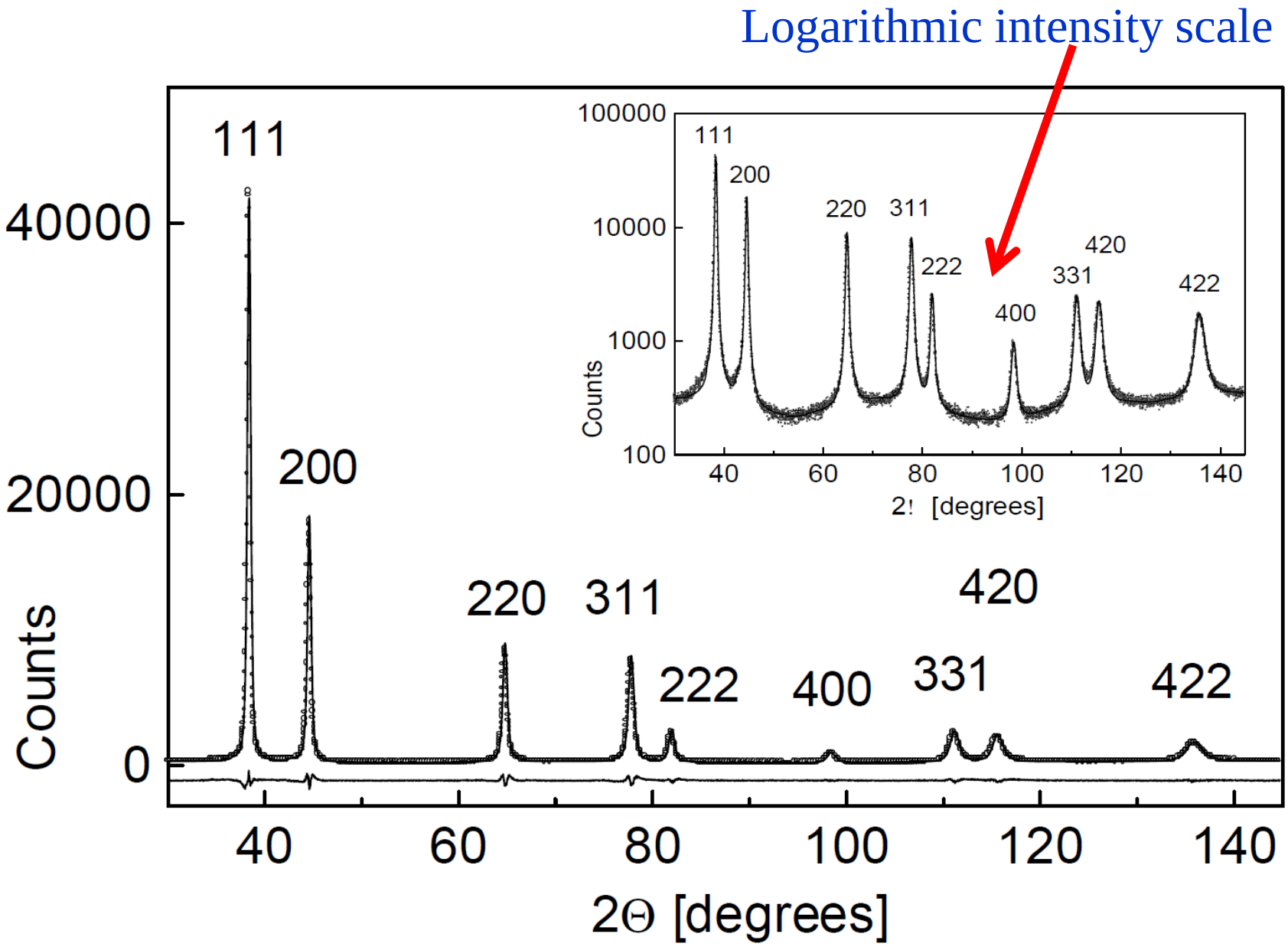

ZK60 Mg alloy deformed by **ECAP**

L. Balogh, R.B. Figueiredo, T. Ungár, T.G. Langdon, *Mater. Sci. Eng. A*, 528 (2010) 533-538.

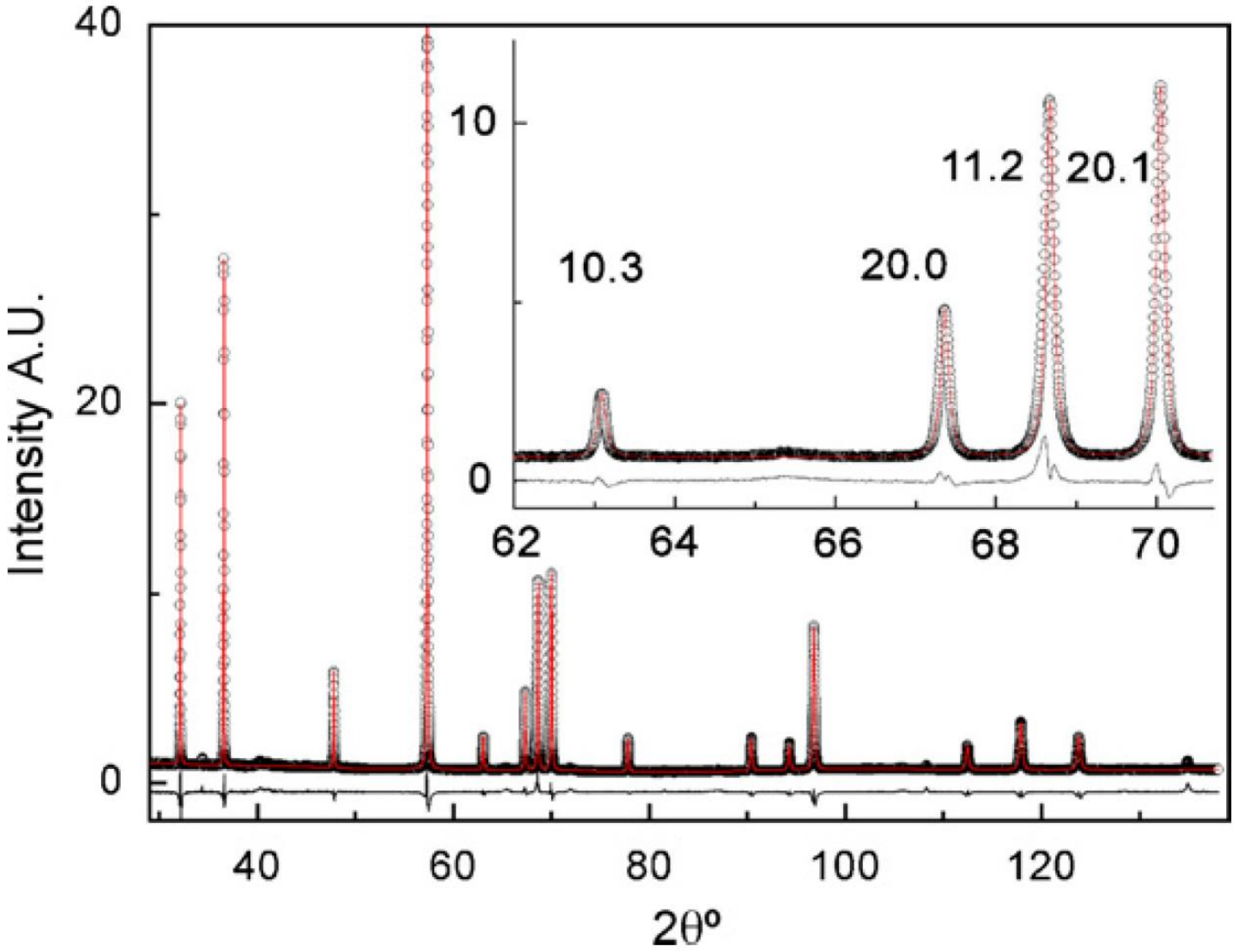

Al-base Al-Mg alloy **friction-stir-welded (FSW)**

W. Woo, L. Balogh, T. Ungár, H. Choo, Z. Feng, *Mater. Sci. Eng. A*, 498 (2008) 308-313.

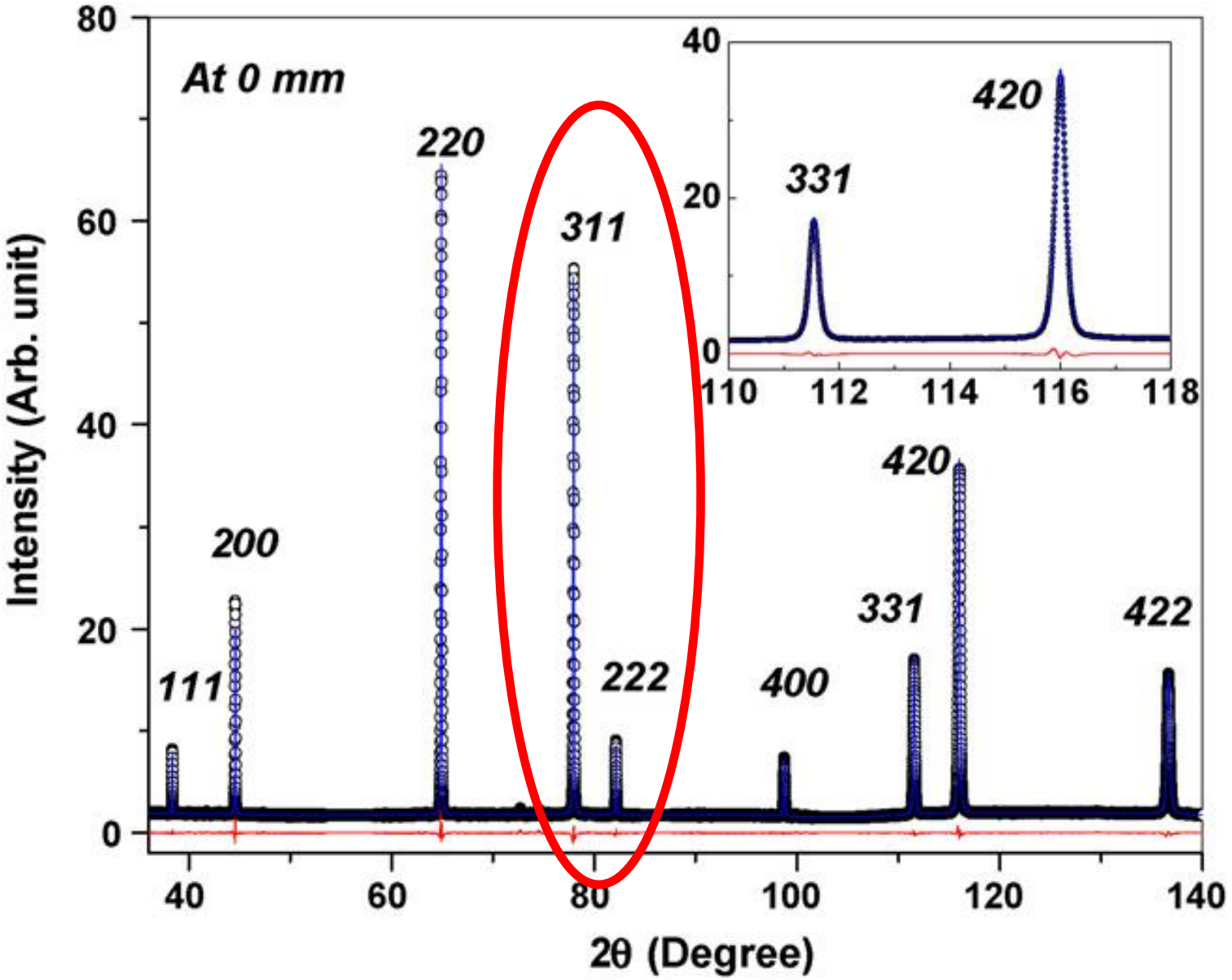

Al-base Al-Mg alloy **friction-stir-welded (FSW)**

W. Woo, L. Balogh, T. Ungár, H. Choo, Z. Feng, *Mater. Sci. Eng. A*, 498 (2008) 308-313.

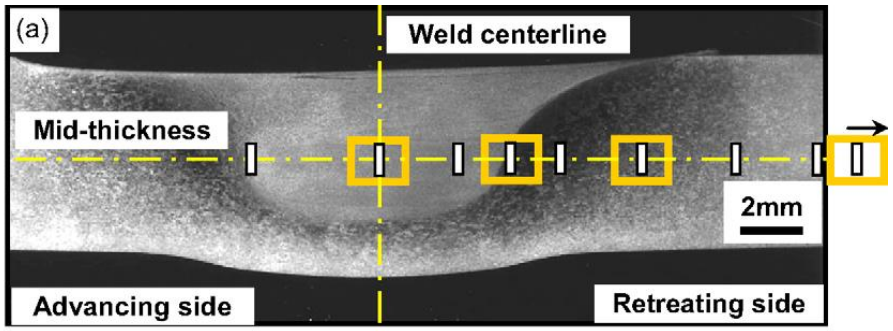

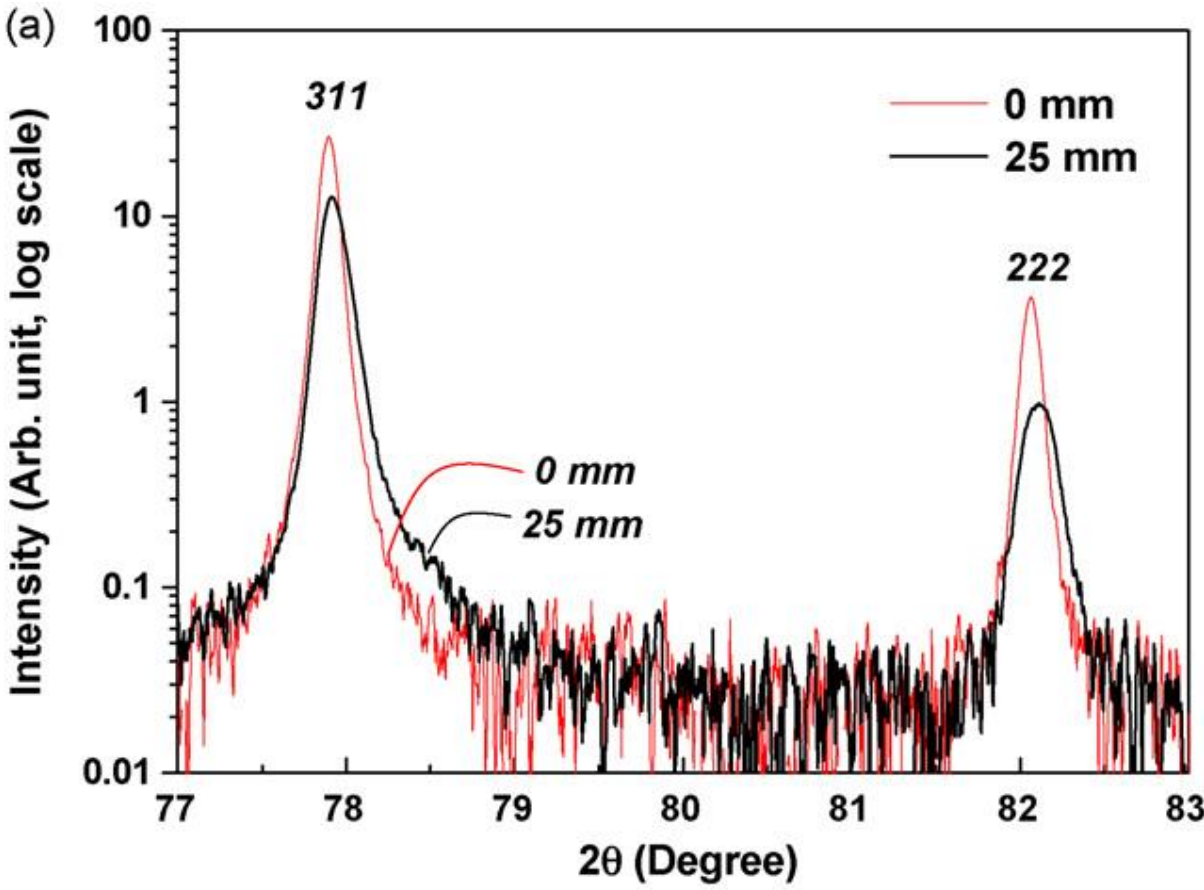

Fortunately the instrumental effect

- can be **small**

- can be **corrected**, **if necessary**

Diffraction from „**perfect**” crystals of **LaB_6**

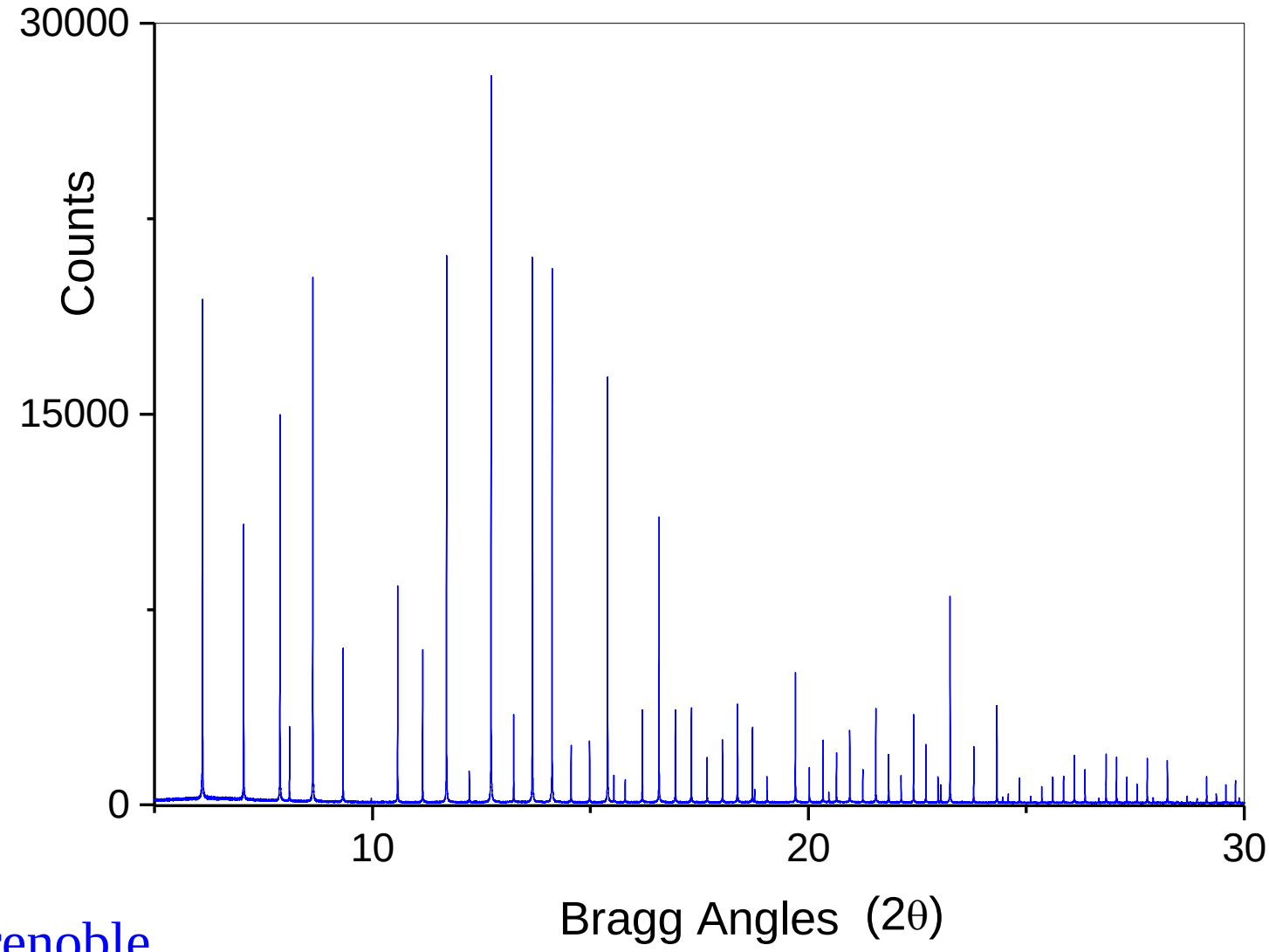

ESRF - Grenoble

Diffraction from **PbS - Galena**, **grinded** for 12 hours

T. Ungár, P. Martinetto, G. Ribárik, E. Dooryhée, Ph. Walter, M. Anne, J. Appl. Phys. 91 (2002) 2455-2465.

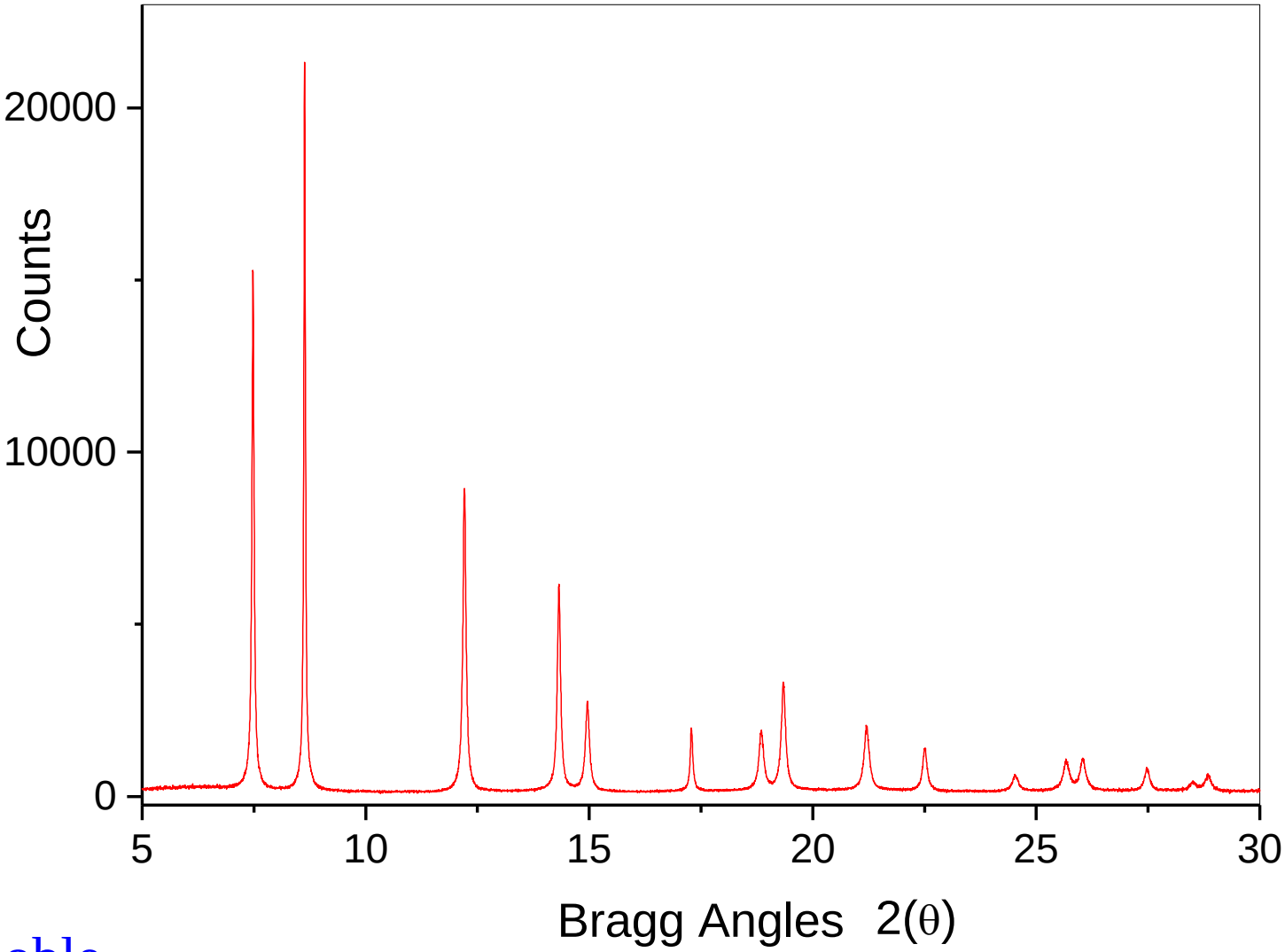

ESRF - Grenoble

The **difference** betwee the **Measured** and the **Instrumental** profiles **tells** us the **microstructure**

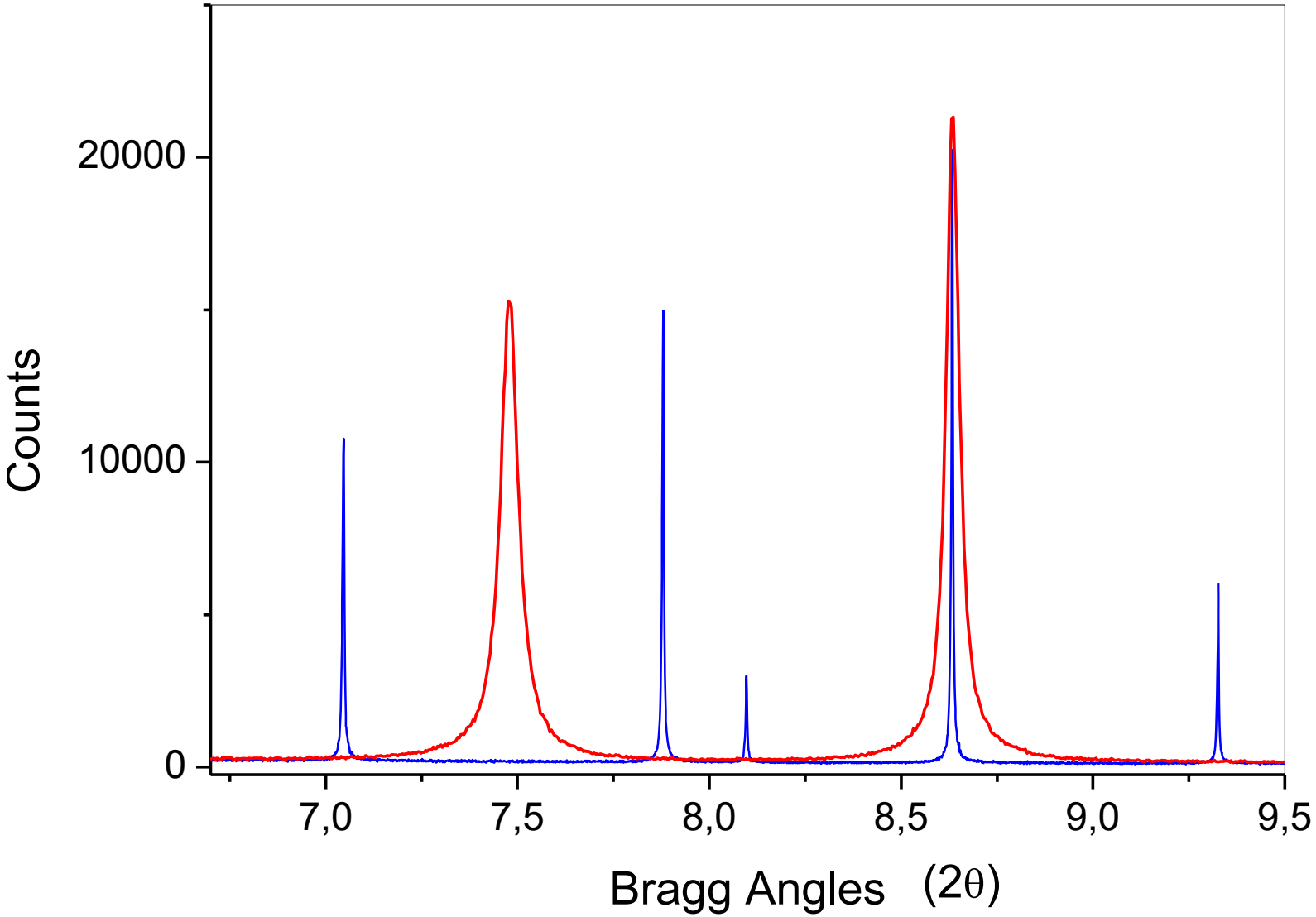

X-ray diffraction peaks can

- be shifted
- can broaden
- can become asymmetric
- can have any combination of these three

[001] Cu single crystals deformed in tension

T.Ungár, H.Mughrabi, D.Roennpagel, M.Wilkens, *Acta Metall.* **32** (1984) 333.

H.Mughrabi, T.Ungár, W.Kienle M.Wilkens, *Phil. Mag.* **53** (1986) 793.

(i) broadening:
dislocations

(ii) asymmetry:
internal stresses
gradient stresses

(iii) shift:
homogeneous strains
due to **vacancies**

(iv) background
has been subtracted

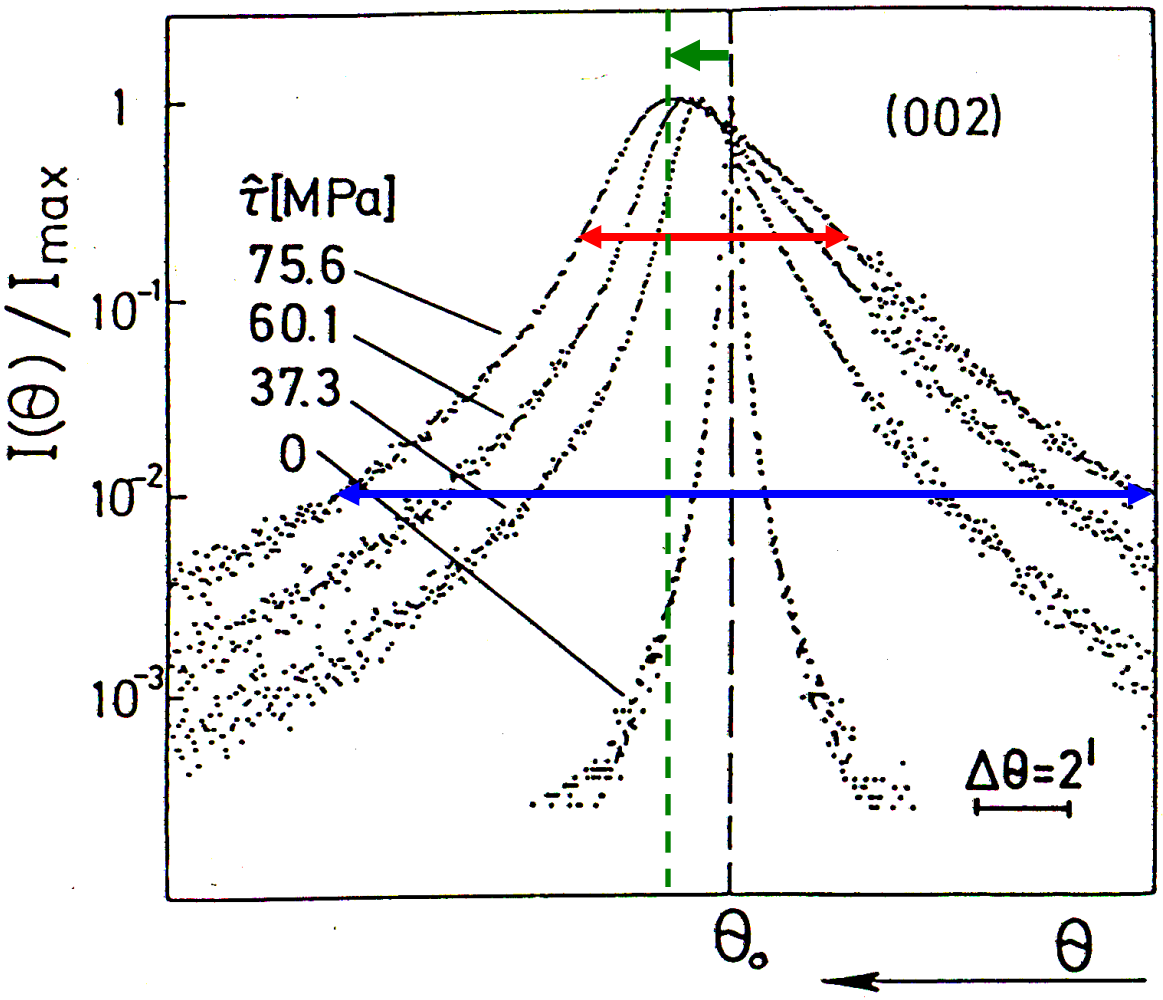

Peak shifts

internal stresses of different kinds
stacking faults,
chemical inhomogeneities

Broadening

microstrains
nanograins
subgrains
small crystallites

Asymmetries

internal stresses of different kinds
stacking faults,
chemical inhomogeneities

Separation of the different effects is based on

- order dependence

- *hkl* anisotropy

- profile-shape

- sub-profile displacement

Schematic picture of line broadening

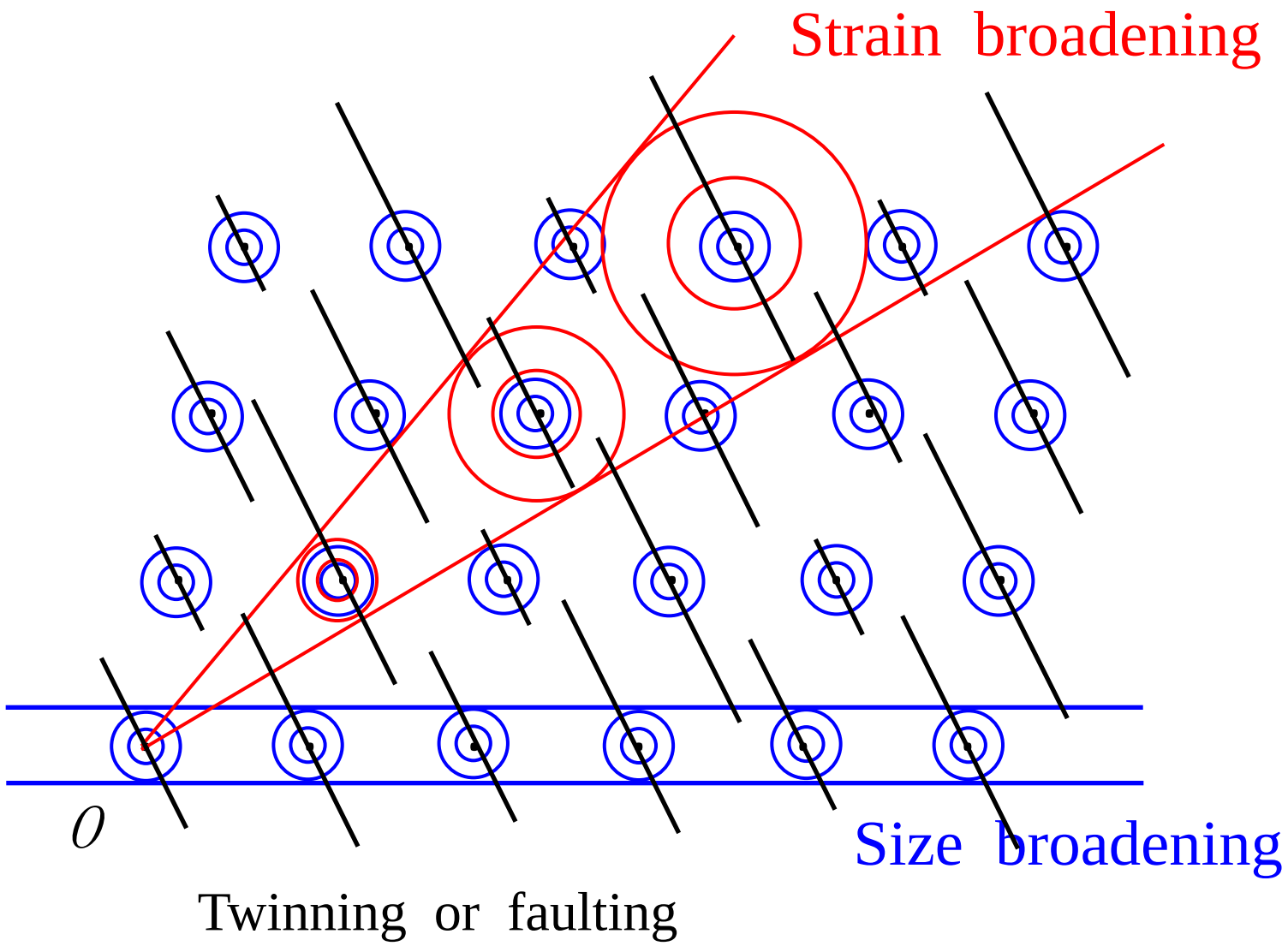

Two different approaches - philosophies:

top-down

bottom-up

Top-down:

the diffraction patterns are

fitted by **analytical** profile-functions

Bottom-up:

the **profile-functions** are

created by **theoretical methods**

based on **actual lattice defects**

diffraction patterns are **fitted** by

these **defect-related profile-functions**

Top-down **analytical** profile-functions:

Analytical Line-Profile Functions

Lorentzian [L]:

$$I(x) = I_o \frac{w^2}{w^2 + x^2}$$

where FWHM = $2w$

Gaussian [G]:

$$I(x) = I_o \exp(-\pi x^2/\beta^2)$$

where $w = \beta [\ln 2/\pi]^{1/2}$

Pearson VII [PVII]:

$$I(x) = I_o \left(\frac{1}{1 + cx^2}\right)^m$$

where m is Pearson VII index and $c = f(w)$ $= (2^{1/m} - 1)/w^2$

([PVII] → [G] as $m \to \infty$)

Pseudo-Voigtian [Ps-Vt]:

$$I(x) = I_o \{\eta [L] + (1-\eta)[G]\}$$

where η is the Lorentzian fraction or Ps-Vt mixing factor

Voigtian [V]:

Convolution of [L] and [G] functions, or

$$[V] = [L] * [G]$$

[See Wiles & Young (1981), JAC 14, 149–151.]

For many good reasons we follow the

bottom-up approach

The hierarchy of non-size-type lattice defects

Krivoglaz: the spatial dependence of strain: $\varepsilon(r)$

0 dimensional: point defects
point-defect-type, e.g. precipitates
inclusions

$\varepsilon(r) \sim 1/r^2$

1 dimensional: **dislocations**
non-equilibrium triple-junctions
linear-type defects

$\varepsilon(r) \sim 1/r$

2 dimensional: planar defects, e.g. stacking faults
twin boundaries
grain boundaries
domain boundaries

$\varepsilon(r) \sim$ constant

crystal-space *versus* reciprocal-space

short distance ⟶ **long** distance

long distance ⟶ **short** distance

Krivoglaz: the spatial dependence of strain: $\varepsilon(r)$

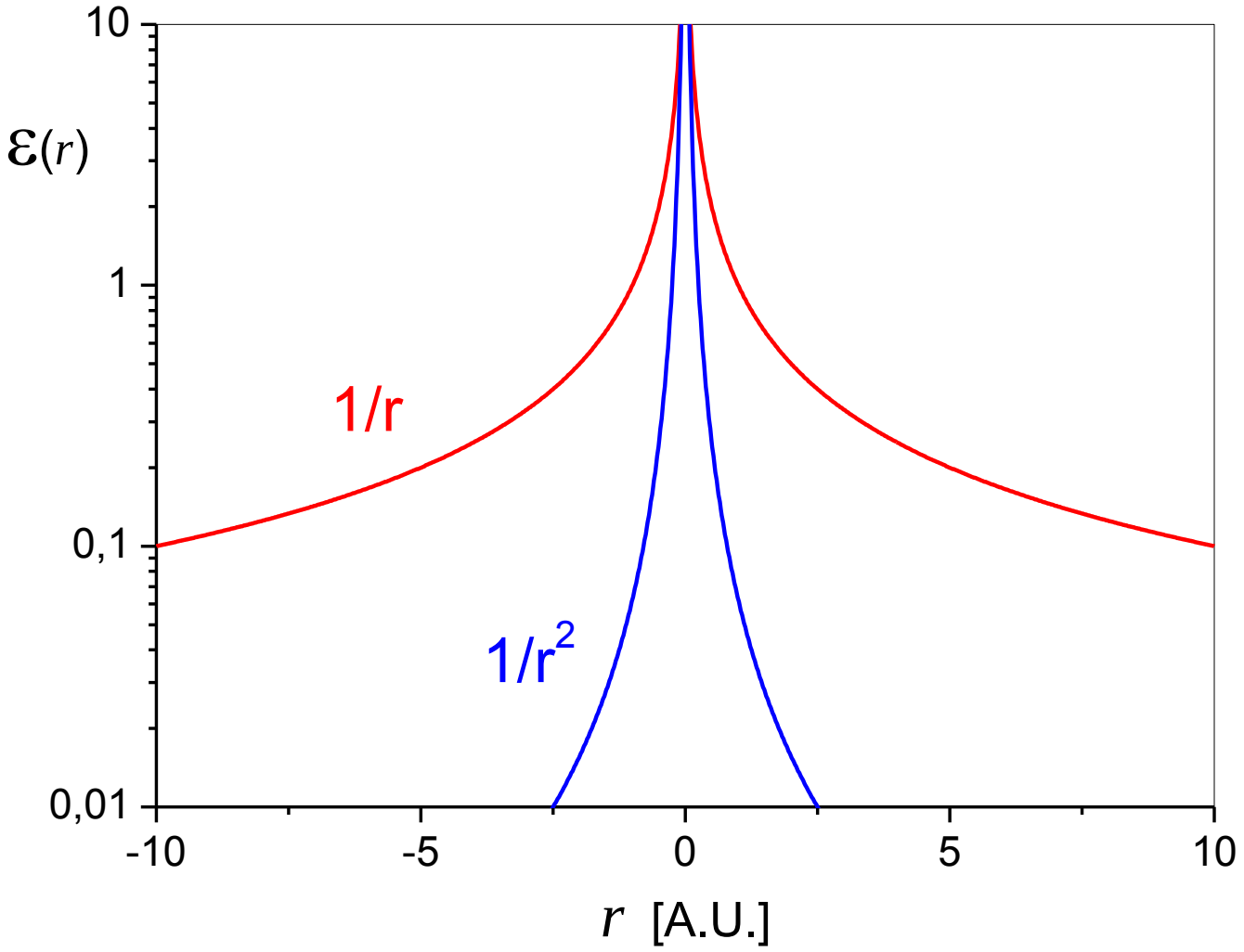

0 dimensional: point defects

point-defect-type, e.g. precipitates

inclusions

$\varepsilon(r) \sim 1/r^2$

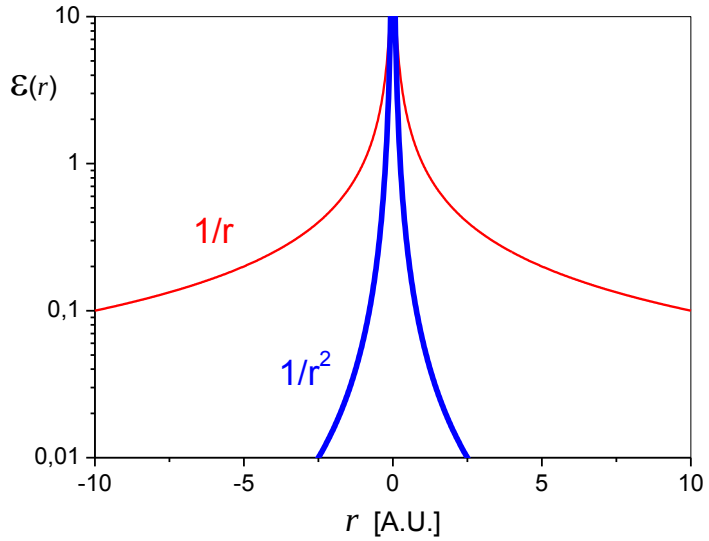

Diffraction pattern: **diffuse scattering**

1 dimensional: **dislocations**

non-equilibrium triple-junctions

linear-type defects

ε(r) ~ 1/r

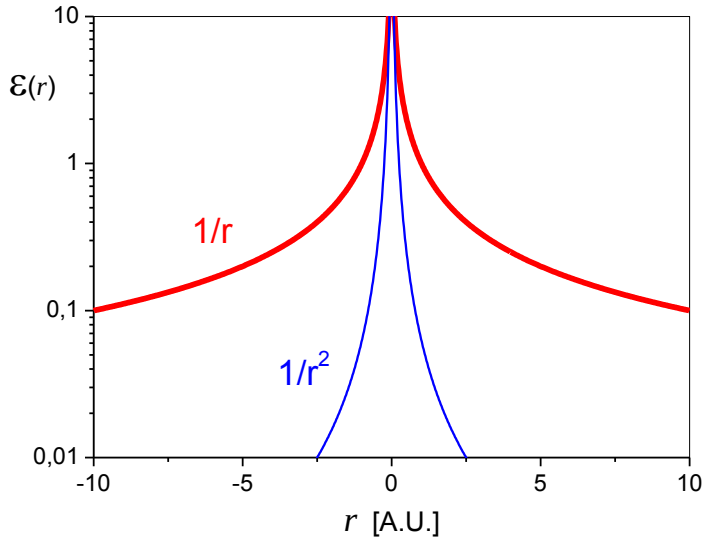

Diffraction pattern: **line broadening**

2 dimensional: planar defects, e.g. stacking faults
twin boundaries
grain boundaries
domain boundaries

ε(r) ~ constant

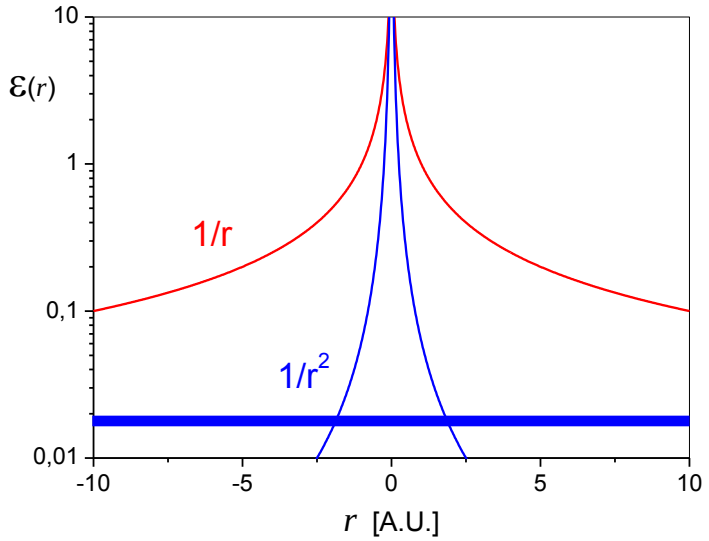

Diffraction pattern: **peak shift**

Line broadening is caused by strain: **if and only if**

strain is produced by **linear-type defects**

the prototype of which are: **dislocations**

Fundamental equation for line-broadening: Warren [1958]:

$$A_L(g) \cong A_L^S \exp\{ - 2\pi^2 L^2 g^2 \langle \varepsilon_g^2 \rangle \}$$

Strain Fourier coefficients

Dislocation-model for $\langle \varepsilon_{g,L}^2 \rangle$: **Wilkens** [1970]:

$$\langle \varepsilon_{L,g}^2 \rangle = \frac{\rho \cdot C \cdot b^2}{4\pi} f(\eta)$$

$\boldsymbol{b}$: Burgers vector

ρ : dislocation density

C : Contrast factor of dislocations

$f(\eta)$: Wilkens function [1970]

$$\eta = L/\boldsymbol{R}_e$$

The Wilkens function [1970]

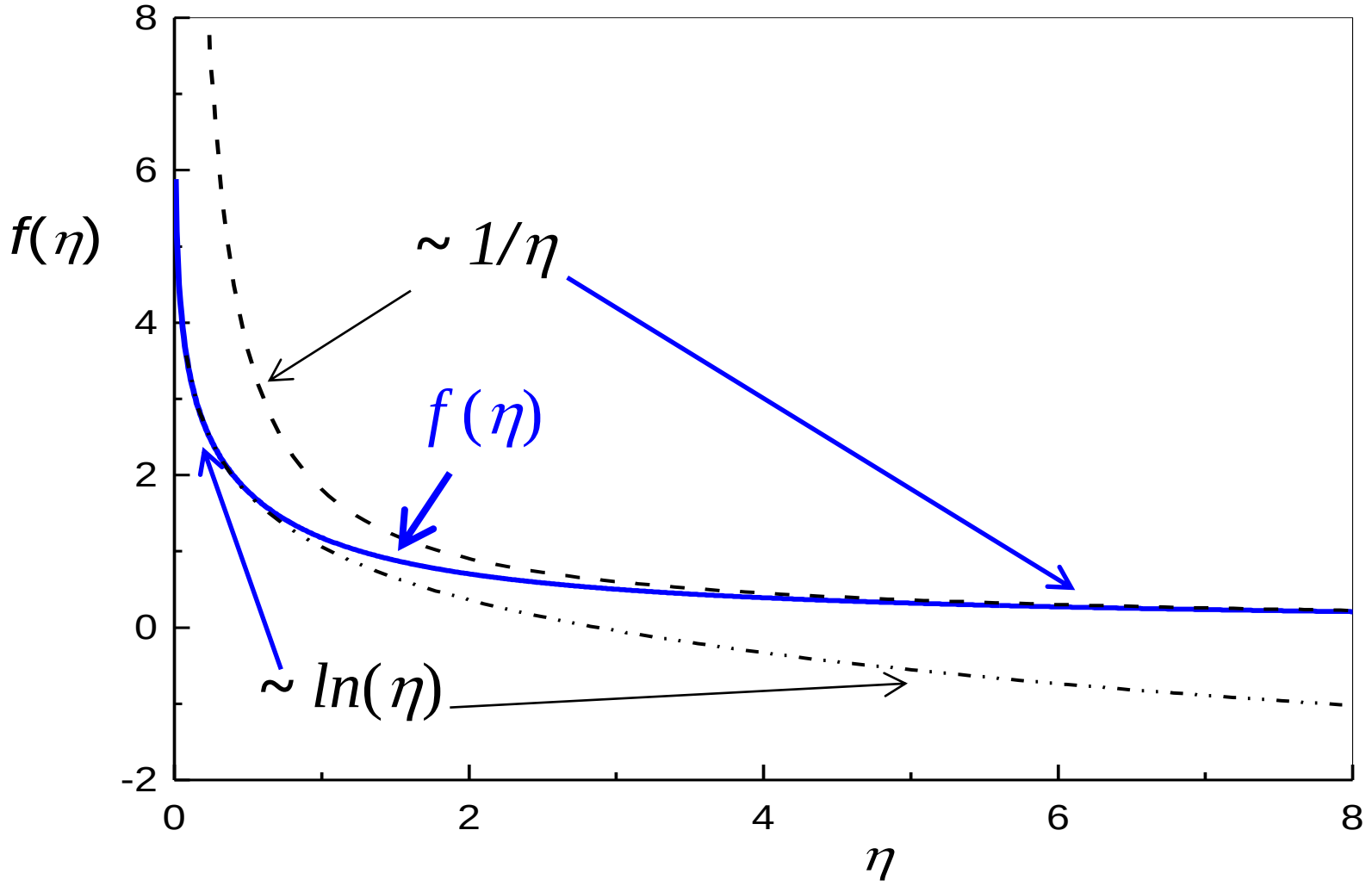

Dislocation **arrangement** parameter

random

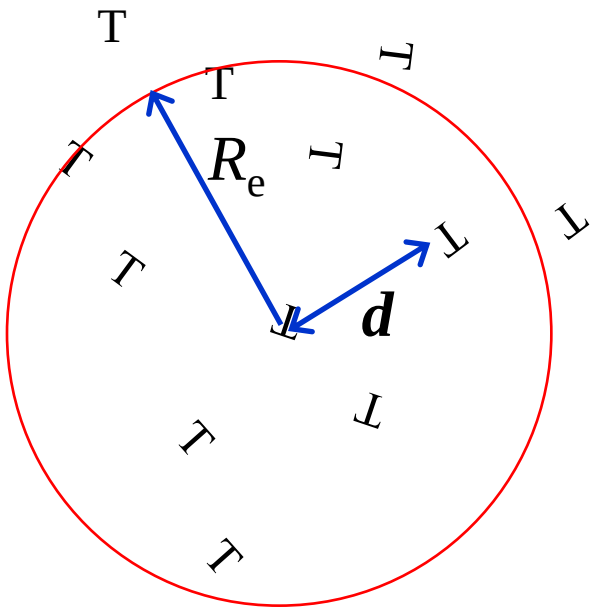

$R_e > d$ $\rho^{1/2}=1/d$

$\boldsymbol{M} = R_e/d = R_e\rho^{1/2} > 1$

highly correlated

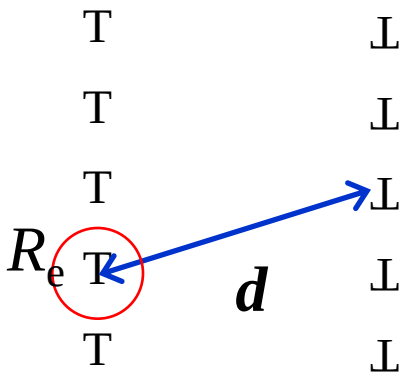

$R_e << d$ $\rho^{1/2}=1/d$

$\boldsymbol{M} = R_e\rho^{1/2} << 1$

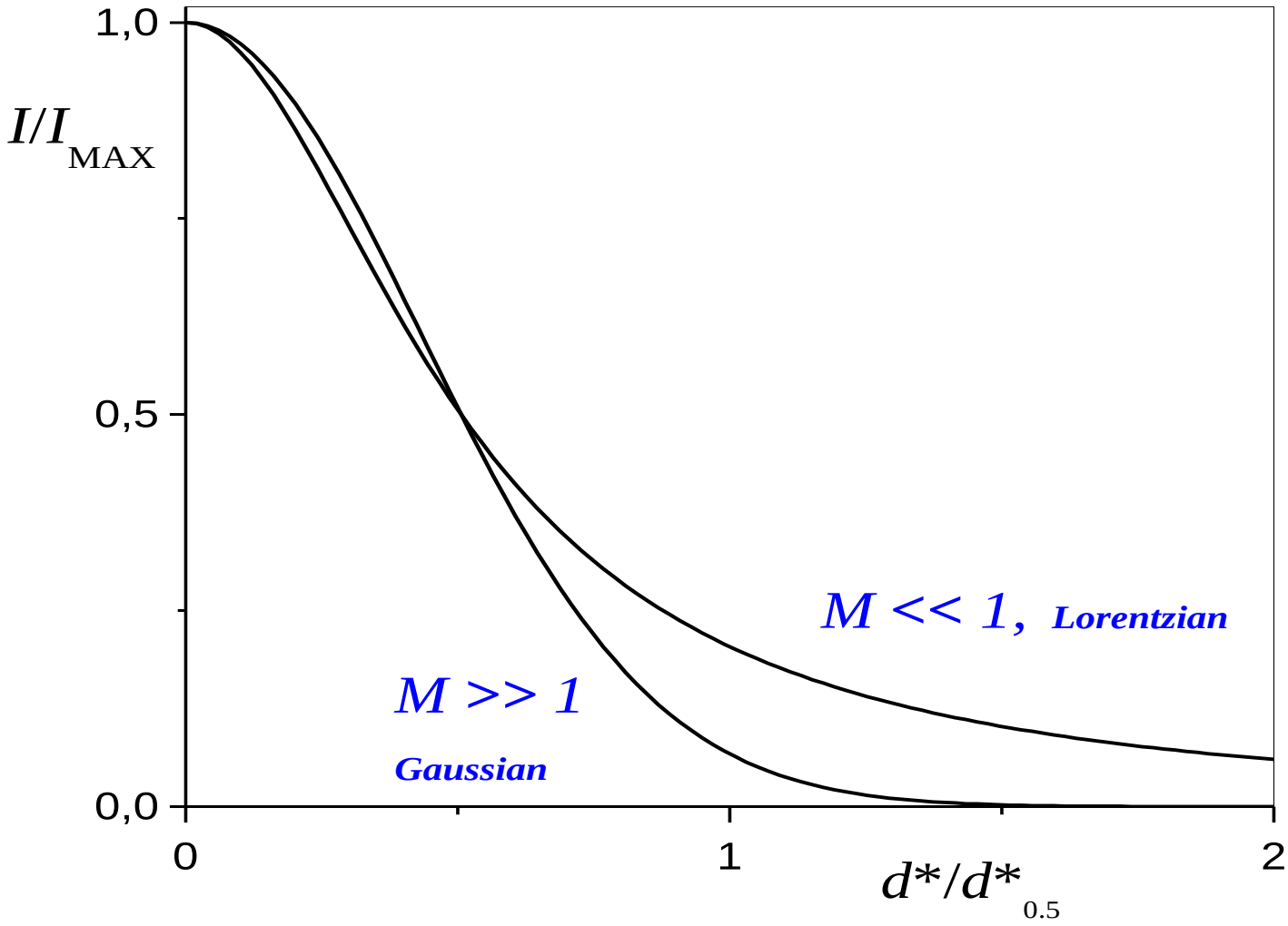
1,0
0,5
0,0
I/I MAX
0
1
2
d*/d* 0.5
M << 1, Lorentzian
M >> 1
Gaussian

Strain profile **3** parameters (in cubic crystals)

dislocation
- density : ρ
- arrangement parameter: M

contrast factor - strain anisotropy: q

Strain profile:

inverse Fourier transform of the *strain Fourier coefficients*

$$I^D(s) = \int \exp\{ - 2\pi^2 L^2 g^2 \langle \varepsilon_{L,\boldsymbol{g}}{}^2 \rangle \} \exp(2\pi i L s) \mathrm{d}L$$

where:

$$\langle \varepsilon_{g,L}{}^2 \rangle = (b/2\pi)^2 \pi\rho \, C \;\; f(\eta)$$

Size profile: I^S

assuming **log-normal** size distribution:

$$f(x) = \frac{1}{(2\pi)^{1/2}\sigma}\frac{1}{x}\exp\left\{-\frac{[\log(x/m)]^2}{2\sigma^2}\right\}$$

m: median

σ: variance

$$I^S(s) = \int_0^\infty \mu \, \frac{\sin^2(\mu\pi s)}{(\pi s)^2} \, \mathrm{erfc}\left[\frac{\log(\mu/m)}{2^{1/2}\sigma}\right] \mathrm{d}\mu$$

CMWP method

Philosophy of evaluation

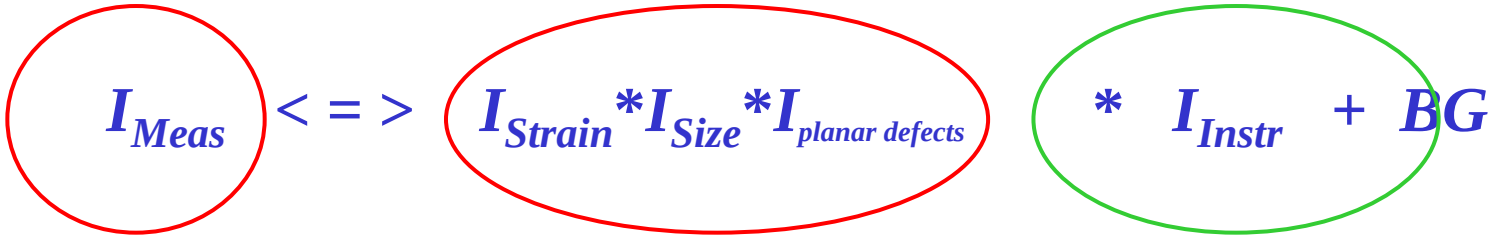

Measured pattern ***Physically modeled*** ***Experimentally determined***

Non-linear, least squares fitting

I_{Strain} : ρ, M, q $\quad M = R_e\rho^{1/2}$

I_{Size} : m, σ

$I_{planas\ defects}$: α or β

In ***cubic*** *crystals altogether:* **5+1** *parameters*

CdF_2 ball milled for 12 min

G. Ribárik, N. Audebrand, H. Palancher, T. Ungár and D. Louër, *J. Appl. Cryst.* (2005). 38, 912–926

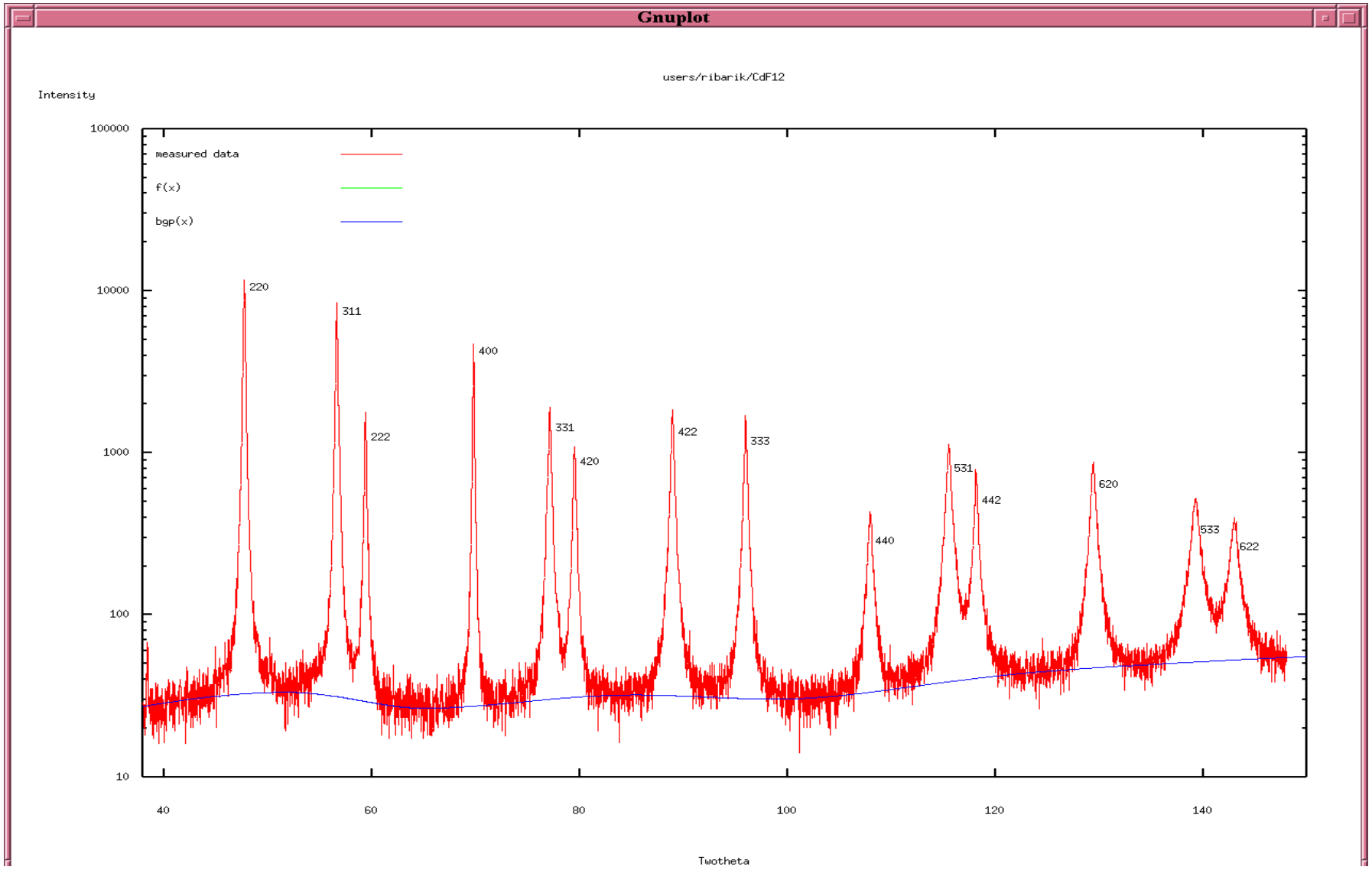

Thank you

for your

attention